A new era for understanding amyloid structures and disease

Matthew G. Iadanza[1,2], *Matthew P. Jackson*[1,2], *Eric W. Hewitt*[1], *Neil A. Ranson*[1] *and Sheena E. Radford*[1]*

Abstract | The aggregation of proteins into amyloid fibrils and their deposition into plaques and intracellular inclusions is the hallmark of amyloid disease. The accumulation and deposition of amyloid fibrils, collectively known as amyloidosis, is associated with many pathological conditions that can be associated with ageing, such as Alzheimer disease, Parkinson disease, type II diabetes and dialysis-related amyloidosis. However, elucidation of the atomic structure of amyloid fibrils formed from their intact protein precursors and how fibril formation relates to disease has remained elusive. Recent advances in structural biology techniques, including cryo-electron microscopy and solid-state NMR spectroscopy, have finally broken this impasse. The first near-atomic-resolution structures of amyloid fibrils formed in vitro, seeded from plaque material and analysed directly ex vivo are now available. The results reveal cross-β structures that are far more intricate than anticipated. Here, we describe these structures, highlighting their similarities and differences, and the basis for their toxicity. We discuss how amyloid structure may affect the ability of fibrils to spread to different sites in the cell and between organisms in a prion-like manner, along with their roles in disease. These molecular insights will aid in understanding the development and spread of amyloid diseases and are inspiring new strategies for therapeutic intervention.

Amyloid
Fibrils formed from proteins, marked by a characteristic cross-β organization with an ~4.7–4.8 Å repeat running down the fibril axis.

Cross-β
The structural motif consisting of β-strands organized perpendicular to the axis of a fibril and stabilized by inter-strand hydrogen bonds and dry steric zipper interfaces between adjacent β-sheets.

[1]*Astbury Centre for Structural Molecular Biology, School of Molecular and Cellular Biology, Faculty of Biological Sciences, University of Leeds, Leeds, UK.*

[2]*These authors contributed equally: Matthew G. Iadanza, Matthew P. Jackson.*

**e-mail: s.e.radford@leeds.ac.uk*

https://doi.org/10.1038/s41580-018-0060-8

Despite the first observation of amyloid deposits nearly four centuries ago[1] (FIG. 1), it has been a long wait to see the structures of amyloid fibrils associated with devastating conditions such as Alzheimer disease (AD) and Parkinson disease (PD) in atomic detail. However, in the past 2 years fibril structures have been determined in near-atomic detail, thanks to developments in methods to create fibrils in vitro, or to purify them from ex vivo material, as well as breakthroughs in cryo-electron microscopy (cryo-EM) and solid-state NMR spectroscopy (ssNMR). Together, these methods have revealed the structures of amyloid fibrils implicated in some of the gravest of human diseases — amyloid-β (Aβ)40/42 and tau associated with AD[2,3] and α-synuclein associated with PD[4]. Although, as expected, the fibrils adopt the canonical cross-β structure of amyloid (see below), these fibrils are more complex and elaborate than suspected previously, suggesting that a wide variety of amyloid structures exists, reminiscent perhaps of the different organization of α-helices and β-strands in globular proteins (1,375 distinct folds in globular proteins have been identified to date[5]). Such diversity may explain why amyloid diseases are so difficult to understand and to treat, with different clinical presentations, even when aggregation of the same protein is the culprit. Understanding the molecular architecture of amyloid fibrils may be an important step towards development of therapeutic interventions based on targeting the fibrils themselves or the processes that generate them.

Approximately 50 different proteins or peptides are currently known to assemble into amyloid fibrils associated with human disease[6] (TABLE 1). These precursors, each with a different primary sequence, self-assemble into amyloid fibrils that accumulate into extracellular plaques and intracellular inclusions associated with disease, which are especially prevalent during ageing[7,8]. Emerging evidence has shown that intracellular inclusions of amyloid can interfere with cellular physiology, for example, by disrupting transport of proteins and RNA[9] and by sequestering chaperones and proteasomes[10]. Plaques from different phenotypic forms of the same disease can also accumulate different proteins[11] and non-protein components[12,13] to varying extents, potentially providing clues to the different phenotypes observed within an amyloid disease.

Amyloid fibrils share a common underlying architecture, in which the β-strands within each protofilament align perpendicular to the long axis of the fibril, termed a cross-β amyloid fold (FIG. 2) marked by a characteristic ~4.7–4.8 Å repeat running down the fibril axis.

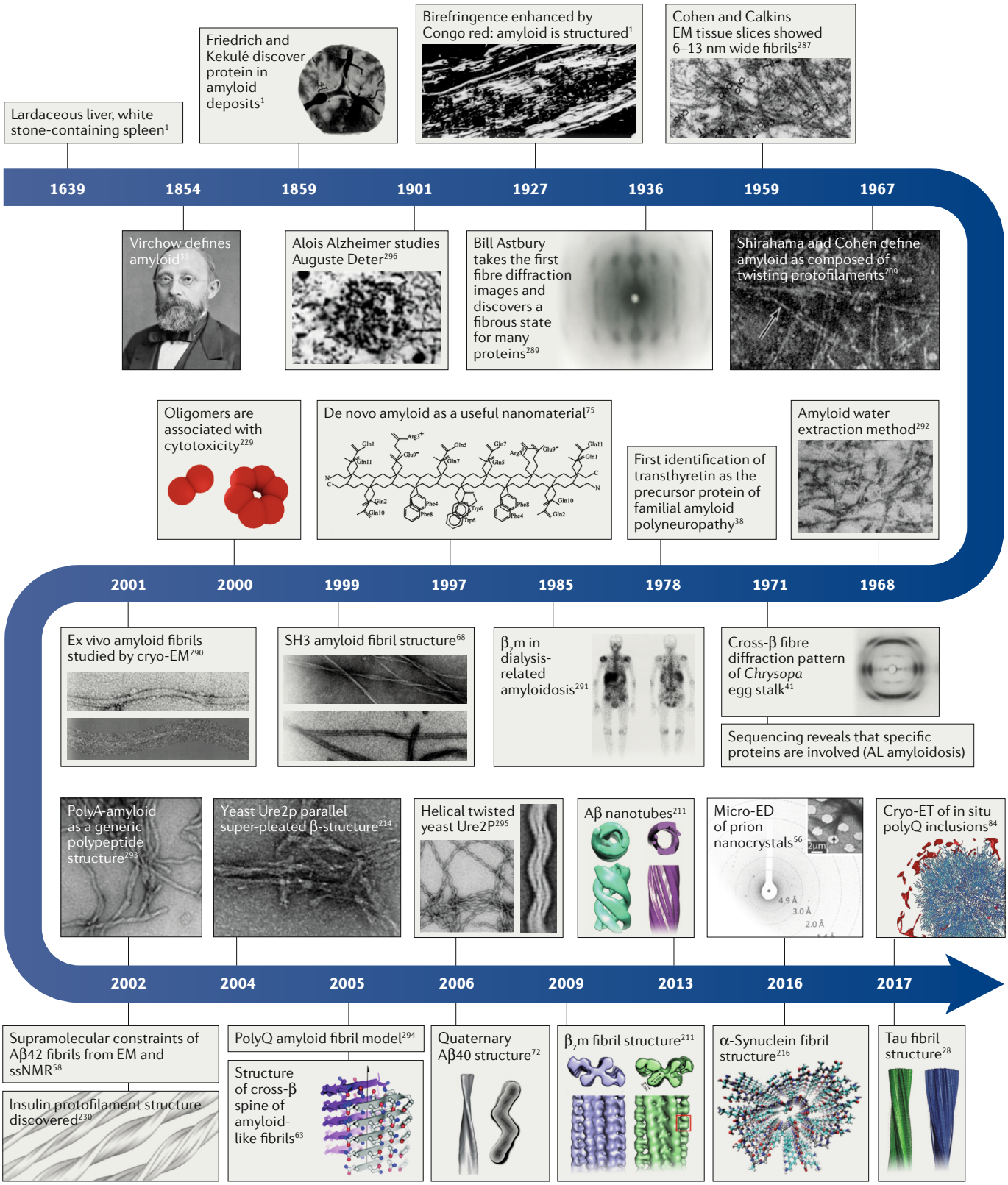

Fig. 1 | **Progression of amyloid structure research over close to 400 years that has culminated in the first atomic structures of amyloid fibrils.** The timeline displays the history of key discoveries in the amyloid field from the initial identification of amyloid to discoveries that led to the first structures of amyloid fibrils associated with disease in all-atom detail[288–296]. Aβ, amyloid-β; β_2m, β_2-microglobulin; cryo-EM, cryo-electron microscopy; cryo-ET, cryo-electron tomography; EM, electron microscopy; micro-ED, micro-electron diffraction; polyA, poly-alanine; polyQ, poly-glutamine; ssNMR, solid-state NMR spectroscopy. Images reproduced with permission from REF.[288], Cold Spring Harbor Laboratory Press; REF.[289,290], Elsevier; REF.[291], American Society for Clinical Investigation; REFS[292,294], John Wiley and Sons; REF.[293], American Chemical Society; REFS[295,296], Springer Nature Limited.

Chaperones
Proteins that assist in the folding, unfolding, assembly or disassembly of other macromolecular structures.

Protofilament
A structural component of an amyloid fibril with a cross-β structure that twists together with one or more additional protofibrils to form a mature amyloid fibril.

Subunits
The smallest units that make up an amyloid fibril, generally single copies of the precursor protein.

Amyloidoses
A class of diseases associated with the formation of amyloid fibrils, tangles and plaques, although the causative agents of disease have yet to be determined definitively.

Prion
A class of infectious amyloid fibrils.

This structure has the strength of steel[14,15] and, on the basis of its simplicity and ease of formation, has also been proposed as a potential primordial structure of life[16]. Amyloid can be either functional (in bacteria, fungi and higher eukaryotes)[17–26] or disease-associated (TABLE 1), with both types of fibril sharing the canonical cross-β architecture unique to the amyloid fold.

Here, we first review the history of our understanding of the amyloid fold, reporting a timeline of discovery from the 17th century to the present day (FIG. 1). We then describe our current understanding of amyloid fibril structure, inspired by recent reports of fibrils formed from proteins associated with human disease[27,28]. We also discuss how amyloid forms and the relationship between protein sequence, fibril morphology and plaque formation, including how these affect disease presentation and progression. Finally, despite recent high-profile setbacks in developing drugs to treat amyloid diseases[29–32], we speculate on how this new, atom-precise vision of amyloid may transform our efforts to treat disease.

Fibril formation and disease

Our understanding of how amyloid fibrils relate to their associated diseases has expanded rapidly in recent years, but from the initial identification of amyloid to the atomic models we have today has been a journey over nearly 400 years.

A timeline of amyloid discovery. First described in 1639 as lardaceous liver and 'white stone'-containing spleen[1], the term amyloid (derived from *amylum* and *amylon*, the Latin and Greek words for starch, respectively), was coined ~200 years later by Virchow on the basis of his discovery that these deposits stained positively with iodine[1,33]. Just 5 years after its misidentification as a polysaccharide, Friedrich and Kekulé showed that amyloid is predominantly proteinaceous[1], with carbohydrates, specifically glycosaminoglycans, being ubiquitously associated with these deposits[34]. Developments in light microscopy, combined with the finding that amyloid deposits show the unique tinctorial property of red–green birefringence in the presence of Congo red[35], revealed that amyloid is formed of highly organized protein subunits. The identification of amyloid A[36] (in 1971), antibody light chains[37] (in 1971) and transthyretin (TTR)[38] (in 1978) as the major protein component of fibrils in plaques showed that an individual protein precursor can be responsible for an amyloid disease. In the meantime, Bill Astbury's pioneering X-ray fibre diffraction studies had shown that amyloid-like fibrils could be created from normally globular, soluble proteins by denaturing them in vitro[39], opening the door to synthetic materials that Astbury hoped would replace wool[40]. In 1968, Sandy Geddes, Bill Aiken and colleagues, working in Astbury's Department of Biophysics at the University of Leeds, UK, used X-ray fibre diffraction to reveal that the egg stalk of the lacewing fly also has a distinct ~4.7 Å repeating feature down the fibril axis, which they named cross-β[41]. This ground-breaking work established a structural fingerprint for amyloid and showed that amyloid is not simply associated with disease (TABLE 1) but can also perform physiological functions in an organism[42–47].

In the 50 years since Geddes et al. coined the term cross-β[41], information about the structure of amyloid fibrils has been drip-fed to the scientific community, with tantalizing insights coming from studies of fibrils formed from short peptides using X-ray fibre diffraction[48], X-ray crystallography[49–51], micro-electron diffraction (micro-ED)[52] of microcrystals[53–56], ssNMR[57–66], cryo-EM[27,28,67–72] and other methods (BOX 1). The ability to assemble fibrils in vitro from synthetic peptides[73–75] and naturally occurring amyloidogenic proteins and peptides[76–78], or from proteins not associated with functional amyloid or disease[68,79], has fuelled developments from each structural technique. However, some of the most recent and exciting breakthroughs have been enabled by the step change in the resolving power of cryo-EM that is currently revolutionizing structural biology[80] (BOX 2). Combining these techniques has finally cracked the amyloid fold, revealing structures that are as beautiful and intricate as those of their globular counterparts[27,28]. These structures give us the first glimpse of how individual protein subunits form cross-β structure, and by combining these data with insights from super-resolution microscopy[81,82], cryo-electron tomography (cryo-ET)[13,83,84] and ssNMR[85], we are entering a new era of integrative structural biology that allows us to 'see' the structure of amyloid fibrils on multiple scales, from individual subunits and how they form fibrils to the cellular consequences of fibril deposition into plaques and tangles.

Diseases associated with amyloid fibril deposition. Alois Alzheimer reported the first documented case of AD in his patient, Auguste Deter, whom he first encountered in 1901 (REFS[86,87]) (FIG. 1). This work, which included the post-mortem visualization of Congo-red-positive plaques in the brain, added AD to the growing list of amyloidoses. Today, more than 50 disease-causing amyloidogenic proteins have been identified, which give rise to an even greater number of diseases depending on the sequence of the precursor and the site of amyloid deposition[88–90] (TABLE 1). These diseases include neurodegenerative disorders such as AD (involving aggregation of Aβ[91] and/or tau[2]), Creutzfeldt–Jakob disease (CJD; prion protein (PrP))[92], Huntington disease (huntingtin[93]), PD (α-synuclein[94]) and amyotrophic lateral sclerosis (ALS; superoxide dismutase (SOD), TAR DNA-binding protein 43 (TDP43) and others[95]). Amyloid disorders affect other tissues: type II diabetes involves the aggregation of amylin (otherwise known as islet amyloid polypeptide (IAPP)[96]) in the islets of Langerhans; in AL amyloidosis, antibody light chains are deposited in the kidney and heart[97]; and in dialysis-related amyloidosis, β_2-microglobulin (β_2m) forms amyloid plaques in the osteoarticular tissues[98]. There is also crosstalk between amyloid diseases. For example, patients with type II diabetes have a higher risk of AD[99], and the non-amyloid component (NAC) of α-synuclein has been found in the plaques of patients with AD[100].

What initiates the onset of amyloid disease remains unclear. Many of the diseases are associated with ageing and involve the aggregation of wild-type proteins,

Table 1 | **Protein precursors associated with amyloid disease**

Disease	Aggregating protein or peptide	Number of amino acids	Native structure of protein or peptide
Neurodegenerative diseases			
Alzheimer disease	Amyloid-β peptide	40 or 42	Natively unfolded
Familial encephalopathy with neuroserpin inclusion bodies	Neuroserpin	410	α + β
Various neurodegenerative disorders	Actin	~400	Mostly α, some β
Neuroferritinopathy	Ferritin	175 or 183	All α
Spongiform encephalopathies	Prion protein or fragments thereof	253	Natively unfolded (residues 1–120) and α-helical (residues 121–230)
Parkinson disease	α-Synuclein	140	Natively unfolded
Dementia with Lewy bodies	α-Synuclein	140	Natively unfolded
Frontotemporal dementia with Parkinsonism	Tau	352–441	Natively unfolded
Amyotrophic lateral sclerosis	Superoxide dismutase	153	All β, immunoglobulin-like
Huntington disease	Huntingtin with polyQ expansion	3,144	The polyQ-containing region is largely unstructured
Spinocerebellar ataxias	Ataxins with polyQ expansion	816	All β, AXH domain (residues 562–694); the rest are unknown
Spinocerebellar ataxia 17	TATA box-binding protein with polyQ expansion	339	α + β, TBP-like (residues 159–339); unknown (residues 1–158)
Spinal and bulbar muscular atrophy	Androgen receptor with polyQ expansion	919	All α, nuclear receptor ligand-binding domain (residues 669–919); the rest are unknown
Hereditary dentatorubral-pallidoluysian atrophy	Atrophin 1 with polyQ expansion	1,185	Unknown
Familial British dementia	ABri	23	Natively unfolded
Familial Danish dementia	ADan	23	Natively unfolded
Non-neuropathic systemic amyloidoses			
AL amyloidosis	Immunoglobulin light chains or fragments	~90	All β, immunoglobulin-like
AH amyloidosis	Immunoglobulin heavy chains or fragments	~220	All β, immunoglobulin-like
AA amyloidosis	Fragments of serum amyloid A protein	76–104	All α, unknown fold
Familial Mediterranean fever	Fragments of serum amyloid A protein	76–104	All α, unknown fold
Senile systemic amyloidosis	Wild-type transthyretin	127	All β, prealbumin-like
Familial amyloidotic polyneuropathy	Mutants of transthyretin	127	All β, prealbumin-like
Haemodialysis-related amyloidosis	β_2-Microglobulin	99	All β, immunoglobulin-like
ApoAI amyloidosis	N-terminal fragments of ApoAI	80–93	Natively unfolded
ApoAII amyloidosis	N-terminal fragment of ApoAII	98	Unknown
ApoAIV amyloidosis	N-terminal fragment of ApoAIV	~70	Unknown
ApoCII amyloidosis	ApoCII	79	α + unstructured
ApoCIII amyloidosis	ApoCIII	79	α + unstructured
Finnish hereditary amyloidosis	Fragments of gelsolin mutants	71	Natively unfolded
Lysozyme amyloidosis	Mutants of lysozyme	130	α + β, lysozyme fold
Fibrinogen amyloidosis	Variants of fibrinogen α-chain	27–81	Unknown
Icelandic hereditary cerebral amyloid angiopathy	Mutant of cystatin C	120	α + β, cystatin-like
Non-neuropathic localized diseases			
Type II diabetes	Islet amyloid polypeptide (also known as amylin)	37	Natively unfolded
Aortic media amyloidosis	Lactadherin C2-like domain	50	Unfolded
LECT2 amyloidosis	Leukocyte cell-derived chemotaxin 2	151	Unknown
Localized cutaneous amyloidosis	Gelactin 7	136	All β

Table 1 (cont.) | **Protein precursors associated with amyloid disease**

Disease	Aggregating protein or peptide	Number of amino acids	Native structure of protein or peptide
Non-neuropathic localized diseases (cont.)			
Hypotrichosis simplex of the scalp	Corneodesmosin	529 (truncations cause amyloid)	Unknown
Calcifying epithelial odontogenic tumours	Odontogenic ameloblast-associated protein	153	Unknown
Senile seminal vesicle amyloidosis	Semenogelin 1	462	Unknown
Medullary carcinoma of the thyroid	Calcitonin	32	Natively unfolded
Atrial amyloidosis	Atrial natriuretic factor	28	Natively unfolded
Hereditary cerebral haemorrhage with amyloidosis	Mutants of amyloid-β peptide	40 or 42	Natively unfolded
Pituitary prolactinoma	Prolactin	199	All α, four-helical cytokines
Injection-localized amyloidosis	Insulin	21 + 30	All α, insulin-like
Injection-localized amyloidosis	Enfuvirtide	36	Unstructured
Aortic medial amyloidosis	Medin	50	Unknown
Hereditary lattice corneal dystrophy	Mainly C-terminal fragments of kerato-epithelin	50–200	Unknown
Corneal amyloidosis associated with trichiasis	Lactoferrin	692	α + β, periplasmic-binding protein like II
Cataract	γ-Crystallins	Variable	All β, γ-crystallin like
Calcifying epithelial odontogenic tumours	Unknown	~46	Unknown
Pulmonary alveolar proteinosis	Lung surfactant protein C	35	Unknown
Inclusion-body myositis	Amyloid-β peptide	40 or 42	Natively unfolded
Cutaneous lichen amyloidosis	Keratins	Variable	Unknown

Each protein precursor is listed, alongside the size and structure of the precursor and the disease with which it is associated. Data were taken from REFS[6,88].
ABri, British amyloid; AD, Alzheimer disease; ADan, Danish amyloid; APO, apolipoprotein; polyQ, poly-glutamine; TBP, TATA-binding protein.

including most cases of PD and AD[8]. Owing to the ageing of the human population, the estimated economic burden in Europe from AD and PD alone is estimated to rise to €357 billion by 2050 (REF.[101]), comparable to the gross domestic product (GDP) of Austria in 2016. Mutations in amyloidogenic precursors, such as the α-synuclein variants A30P or A53T in PD[102], the Aβ variants E22Δ or E22K in AD[103] or D76N in β_2m-associated amyloidosis[104], can cause diseases to present earlier (TABLE 1). Other disorders are caused by the expansion of an amyloidogenic sequence, such as the trinucleotide repeat diseases, which result in poly-glutamine (polyQ)-associated ataxias such as Huntington disease[93,105], poly-alanine (polyA) expansions in polyadenylate-binding protein 2 (PABPN1) (REF.[106]) associated with oculopharyngeal muscular dystrophy[107] and dipeptide expansions such as poly-GlyAla in *C9orf72*, the most common genetic form of ALS and frontotemporal dementia[108,109]. The age of onset for people with these diseases is variable, as a critical threshold number of repeats determines their pathogenicity, and the rate of disease onset correlates with the number of repeats[105,110].

Modification of a precursor's primary sequence (for example, truncations by the action of proteases or hyperphosphorylation) can enhance or suppress amyloidogenicity. Trimming the precursor protein can reduce amyloidogenicity, evidenced by the lower risk of AD in patients with an increased ratio of Aβ40 to Aβ42 (REF.[111]). By contrast, proteolysis of apolipoprotein A1 (APOA1) increases the risk of amyloidosis in systemic amyloidosis[112] (TABLE 1), and truncation of the amino-terminal six amino acids of β_2m is observed in dialysis-related amyloidosis[113,114] (TABLE 1). Simply increasing the concentration of the monomeric precursor by gene duplication can also cause disease, with gene duplication, triplication or even quadruplication associated with the early onset of PD[94,115], and patients with trisomy of chromosome 21, which contains the gene encoding amyloid precursor protein (APP; from which Aβ40/42 are derived), have a higher risk of AD[116]. The inability of haemodialysis to remove wild-type β_2m from the serum of patients with renal failure causes an ~50-fold increase in β_2m concentration in the serum[117]. Liquid phase separation[118] may also lead to local increases in concentration leading to fibril formation[119]. Intrinsically disordered proteins have a higher propensity towards coacervation, which may explain why many are amyloidogenic, and cross-β polymerization has been suggested as a driving force in the formation of liquid droplets in vivo[120], which can result in dialysis-related amyloidosis in patients undergoing long-term (>10 years) renal replacement therapy[117]. Finally, amyloidogenicity can be modulated by small molecules such as metabolites or metal ions, by membranes and glycosaminoglycans and by the status of the cell itself (chaperone levels, rate of protein synthesis, etc.), which affect the rate of protein aggregation

Age of onset
The age at which a patient first presents symptoms. For amyloid-associated disorders, this is not necessarily directly correlated with fibril load: high fibril loads may be asymptomatic, whereas low fibril loads may lead to severe symptoms.

Haemodialysis
A dialysis-based filtration treatment that acts to replace kidney function in patients experiencing kidney failure.

Phase separation
A process driven by liquid–liquid demixing, leading to a liquid mixture separating into individual components. In cells, this can lead to localized increased concentration and supersaturation of biological molecules.

Intrinsically disordered proteins
Proteins that lack a fixed or ordered 3D structure.

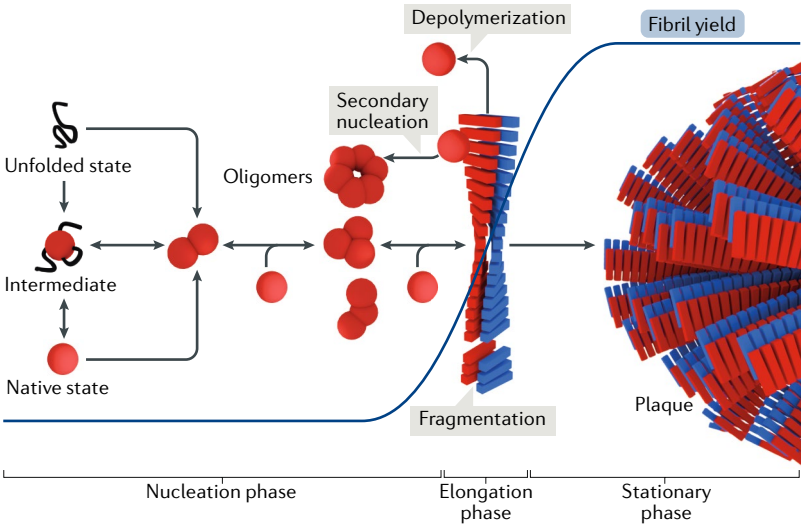

Fig. 2 | **Schematic of amyloid formation.** Native proteins are in dynamic equilibrium with their less-structured, partially folded and/or unfolded states. One (or possibly several) of these states initiates amyloid fibril formation by assembling into oligomeric species. The precursor of aggregation (native, partially folded or unfolded) may differ for different protein sequences. Oligomeric species can then assemble further to form higher-order oligomers, one or more of which can form a fibril nucleus, which, by rapidly recruiting other monomers, can nucleate assembly into amyloid fibrils. This process occurs in the lag time (nucleation phase) of assembly. As fibrils grow, they can fragment, yielding more fibril ends that are capable of elongation by the addition of new aggregation-prone species[140,144,145]. This elongation results in an exponential growth of fibrillar material (blue line) until nearly all free monomer is converted into a fibrillar form. Fibrils are dynamic and can release oligomers that may or may not be toxic[177]. Fibrils can also associate further with each other, with other proteins and with non-proteinaceous factors[188] (not shown here) to form the amyloid plaques and intracellular inclusions characteristic of amyloid disease. Note that any and/or all of these steps are potential points for drug intervention.

and the ability of the cell to respond to the formation of potentially toxic species[9,121].

Prion aggregation and disease. The ability of amyloid to seed its own assembly, causing disease to spread between cells and, in some cases, between organisms, is a hallmark of prion diseases[122,123]. In mammals, PrP causes a family of diseases known as the transmissible spongiform encephalopathies[92]. The soluble α-helical protein, PrP^{C}, can conformationally rearrange to an infectious isoform, PrP^{Sc}, which has β-sheet structure (a process that is not yet understood in atomic detail). As an infectious agent, PrP^{Sc} is believed to be devoid of nucleic acid[124], although this is contested by some studies[125]. There are many prion diseases in humans, such as CJD, familial fatal insomnia, Gerstmann–Sträussler–Scheinker disease and Kuru, which result in different diseases characterized by different age of onset[126]. Bovine spongiform encephalopathy (BSE) in cattle, chronic wasting disease in deer and elk and scrapie in sheep and goats[127] have also been identified as transmissible spongiform encephalopathies. BSE can cross the species barrier to humans, leading to variant CJD (vCJD)[123,124].

Although prion diseases are predominantly neurological, in vCJD, PrP^{Sc} can be found in different tissue types[128]. Prion-like spreading of disease within the brain is not unique to PrP; it is also observed in both PD[129] and AD[130], suggesting that common mechanisms exist by which protein aggregation spreads and causes cell death. In yeast, prion-like spreading of protein aggregates, such as those formed from the proteins Ure2p and Sup35, can be beneficial, endowing metabolic advantages to daughter cells under certain selective pressures[131]. Indeed, the large number of prion-like domains identified in yeast[132] suggest that such selective advantages are commonly adopted, giving enhanced fitness. Despite the prion-like seeding ability of amyloid fibrils, other than in the prionopathies, there is no direct evidence for the spread of amyloid diseases between mammals. There is, however, some evidence for transmissibility of amyloid disease in an experimental setting[133,134]. Thus, it would be wise to treat amyloidogenic proteins and peptides as potential infectious agents.

Mechanisms of fibril and plaque formation

Amyloid is formed by the aggregation of monomeric protein precursors into fibrils by a common nucleation growth mechanism[135,136] (FIG. 2). Monomeric precursors may be unfolded (intrinsically disordered) or partially folded (formed by transient unfolding of a native protein or transient folding of an unfolded protein) (TABLE 1). In rare cases, aggregation may be initiated by the native protein itself[137]. The first step in fibril assembly involves the formation of oligomers, which are dynamic, transient, heterogeneous and of unknown and possibly varied structure[136,138,139]. Oligomers can then further associate to produce higher-order species, which can be either essential precursors of amyloid fibrils (on-pathway) or dead-end assemblies that do not produce fibrils (off-pathway)[136]. Although off-pathway oligomers do not go on to form fibrils, they may still be cytotoxic and relevant to disease. At some stage during oligomerization, a critical nucleus is formed, which is defined kinetically as the most unstable (highest energy) species formed before rapid polymerization into amyloid fibrils. The probability of nucleus formation determines (in part) the length of the lag time of amyloid assembly and possibly the age of disease onset (FIG. 2).

At some point during self-assembly, each precursor undergoes a structural transformation to form β-strand-rich secondary structure, irrespective of its initial fold (TABLE 1). Once fibrils with a cross-β structure form, they can fragment, producing new fibril ends that can recruit monomers, reducing the length of the lag time and resulting in exponential fibril growth[140] (the elongation phase shown in FIG. 2). Other processes, such as secondary nucleation, in which oligomer formation is catalysed on the surface of a pre-existing fibril, also enhance the rate of fibril formation[136,141]. Understanding each process, and how they combine to determine the rate of fibril assembly (and hence fibril load), is vital for elucidation of the mechanism of fibril formation in both in vitro and in vivo environments.

Various models, inspired by work on sickle cell disease by Eaton, Oosawa and colleagues[142,143], including both numerical[140,144] and analytical approaches[145], allow the individual steps of amyloid formation to be kinetically defined by employing simple-to-use algorithms

Native protein
The properly assembled form of a protein required for functionality.

Fibril load
A measure of the total amount of amyloid fibril within a sample or patient.

Crossover
The distance it takes a fibril to achieve 180° of rotation. Crossover appears as the distance between the two narrowest points on a 2D EM or atomic force microscopy image of a twisted fibril.

Long-term potentiation
A persistent increase in synaptic strength after stimulation of the synapse.

now available online[140]. The kinetics of assembly are commonly measured in vitro using the dye thioflavin T (ThT), which binds to amyloid fibrils, generating an enhanced fluorescence signal[145,146]. Using this approach, the effect of synthetic membranes[147], solution conditions[148], molecular chaperones[149], small molecules[150] and the primary sequence[141] on the rate of aggregation can be elucidated. Most importantly, the ability to determine the role of different additives on assembly offers the opportunity to control aggregation by the synergistic application of reagents that target different steps in amyloid formation.

Box 1 | **Techniques that inform on amyloid structure**

Electron microscopy (EM) is by no means the only technique that has driven the understanding of amyloid fibril structure in recent years. A variety of biophysical techniques have been utilized to make advances in understanding fibril structure.

Atomic force microscopy
AFM has been used to examine fibrils adsorbed onto a surface and can report on length distribution, fibril height, width and crossover length. AFM has also been used to track the dynamics of fibrils[275] and oligomers[276] over time.

Solid-state NMR spectroscopy
ssNMR (also referred to as magic angle spinning (MAS) NMR) can be used to determine dihedral angles and inter-atom distances in the subunit of fibrils. These restraints have been used to build atomic models of fibrils[65,66,216,251,277,278] as well as models of the subunit structure, which were then fit into lower-resolution EM models[64,67].

Fluorescent dyes
Fluorescent dyes such as thioflavin T and Congo red have a long history of use identifying amyloid fibrils[35]. More recently, polythiophene dyes have also been shown to have distinct emission wavelengths when bound to different fibril morphologies and can be used to differentiate fibril types[279].

Super-resolution microscopy
Super-resolution microscopy with labelled proteins has been used for high-resolution light microscopy imaging[280] and to observe the addition of monomers to fibril ends, yielding information about fibril polarity and growth[81].

Single-molecule Förster resonance energy transfer
FRET experiments have also been used to track fibril growth and characterize amyloid oligomers[172].

X-ray fibre diffraction
One of the earliest methods used to identify the cross-β motif[41], it is still used, especially as an orthogonal validation technique, as simulated fibre diffraction patterns from a model can be compared with experimental data[281].

X-ray crystallography and micro-electron diffraction
Two methods that have been especially useful to determine the structures of small amyloidogenic peptides; although these peptides usually do not crystallize as fibrils, they have been used to predict the interactions present in the fibrillar form[51,55], to link structure to toxicity[54] and to design inhibitors of fibril formation[272].

Spectroscopy
Methods such as circular dichroism (CD) and Fourier transform infrared (FTIR) can be used to characterize the secondary structure of fibril-forming proteins over time, to track the formation of oligomers and/or fibrils and, in the case of FTIR, to differentiate amyloid from non-amyloid β-sheets[201].

Mass spectrometry
A variety of mass spectrometry (MS) methods have been used to characterize fibrils, including interrogating exposed surfaces via *N*-ethylmaleimide labelling coupled with electrospray ionization MS (ESI-MS)[282] and hydrogen-deuterium exchange (HDX)[283].

Electron paramagnetic resonance
EPR spectroscopy has been used to identify residues involved in the cross-β core of amyloid[284] and to characterize amyloid precursors, oligomers and membrane interactions[285].

Cytotoxicity and implications for disease

Identifying the toxic species formed during amyloid formation, and how they cause cellular dysfunction and death, remains both a challenge and a priority (FIG. 3). Questions abound, including how aggregation is initiated, how aggregates are recognized by chaperones and other cellular components and how and why aggregates saturate the cellular chaperone and degradation networks[151–153]. Models of amyloid-associated cytotoxicity include inhibition of proteasomal degradation[10,151], impairment of autophagy[154], perturbation of mitochondrial function[155], production of reactive oxygen species (ROS)[156], sequestration of other proteins[121] and disruption of membranes, including mitochondria, the endoplasmic reticulum (ER), lysosomes and plasma membrane[84,121,157,158] (FIG. 3).

Crucially, the severity of cognitive decline in patients with AD does not correlate with plaque formation[159], suggesting that pre-amyloid aggregates are the cause of disease[138,139,160–164]. Consistent with this view, numerous experiments in vitro have demonstrated the cytotoxicity of oligomeric species, including their ability to disrupt membranes[165–167]. Oligomers formed from proteins not normally associated with disease can also disrupt membranes and can be cytotoxic, adding weight to the view that oligomers are the causative agents of amyloid-associated cellular dysfunction[162,166–168]. Oligomers formed from disease-related precursors have also been shown to impair memory and long-term potentiation, again supporting their role in disease[169,170]. However, not all oligomers are toxic[171,172]. What is known is that toxic oligomers expose hydrophobic surfaces not found in innocuous precursors or non-toxic counterparts[173], consistent with their ability to perturb membranes and expose the cytoplasm to the extracellular space, causing calcium flux and ultimately cell death[164,174]. The molecular basis for an oligomer's cytotoxicity will remain unclear until a high-resolution structure of a toxic oligomer is solved. However, because oligomers are unstable, dynamic and heterogeneous in mass and structure[175,176], determining their structure–function relationships is challenging.

Recent experiments have re-energized the debate about how, or whether, amyloid fibrils contribute to disease[177]. Using cryo-ET, amyloid fibrils and, in particular, their ends have been shown to perturb artificial lipid membranes (inducing breaks, blebbing and formation of pinched sharp points with high membrane curvature)[178] and to cause pinching of cellular membranes[84], suggesting a role for fibrils in disease. Cryo-ET also showed that intracellular inclusions, formed from exon-1-encoded huntingtin, which contains 97 glutamines, localize to the rough ER, perturbing ER function and dynamics[84]. Interestingly, extracellular assemblies of Aβ42 fibrils in cell culture take distinct forms, including meshworks, semi-parallel bundles and 'stars' radiating out from a central point[13,83]. These extracellular fibrils also interact with membranes, sequestering lipids and forming tubular inclusions at the cell surface[83]. Intracellular inclusions formed by ATG-independent translation of a non-coding region of the ALS-related gene *C9orf72* sequester proteasomes

Box 2 | **Advances in electron microscopy of amyloid fibrils**

Although the use of electron microscopy to examine amyloid fibril structure has a long history[209,286,287], determination of atomic resolution structures became a possibility only with the advent of cryo-electron microscopy (cryo-EM). Cryo-EM led to observation of several fibril structures at intermediate resolutions[68,71,72,210,211,229]. Although this gave information about gross fibril morphology, it could not be used to build atomic models. Only in the past year have cryo-EM structures reached the resolution at which atomic detail can be resolved[27,28]. This advance in resolution has been driven by technological advances in microscope and electron detection equipment and improvements in image processing software[80]. The increase in achievable resolution of cryo-EM reconstructions of fibrils is illustrated with structures of fibrils formed from SH3 domains[68], prion protein (PrP)[210], amyloid-β (Aβ) 1–40 formed in vitro[71] and ex vivo tau[28] (see the figure, parts **a**–**d**).

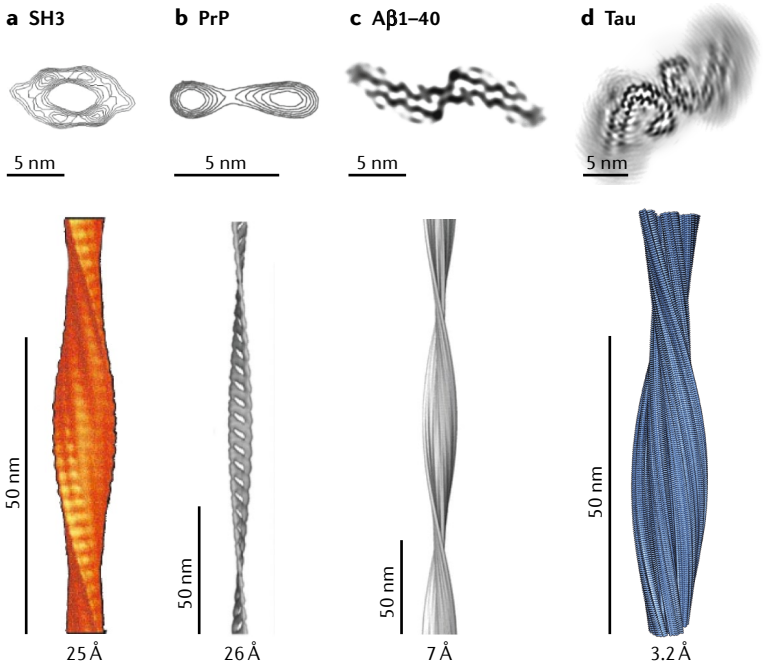

Part **a** adapted with permission from REF.[68], Elsevier. Part **b** adapted with permission from REF.[210], Elsevier. Part **c** adapted with permission from REF.[71] copyright (2008) National Academy of Sciences USA. Part **d** adapted from REF.[28], Springer Nature Limited.

and impair proteasome activity[10], demonstrating that fibrillar assemblies from different proteins have different cellular effects. In support of this view, NMR metabolomics showed that monomeric, oligomeric and fibrillar α-synuclein and Aβ40/42 have different metabolic effects in neuroblastoma cells, suggesting that cells attempt to counter the toxicity imposed by pre-fibrillar species, whereas fibrils led to cellular shutdown[179]. Recent experiments have also shown that different fibril morphologies, even when formed from the same protein, can cause different cellular effects, presumably by binding to different molecules and/or by depositing in different locations[60,180–186]. This is illustrated by Aβ40 fibrils produced in vitro under different conditions. So-called 2A fibrils have two-fold symmetry and were made by seeding from Aβ40 fibrils produced under agitation, whereas fibrils formed from the same protein with three-fold symmetry (named 3Q) were seeded from fibrils produced under quiescent conditions[187]. These Aβ40 fibrils bind the glycosaminoglycan, heparin, with different affinities[12,188], whereas other fibrils bind to specific RNA molecules or other proteins[121].

Finally, the role of fibril structure in disease is being studied. For example, fibrils from brain extracts of patients with AD show distinct size, concentration and conformational characteristics, which correlate with disease duration and severity[189]. This difference in fibril characteristics may in part explain why amyloid fibril load does not always correlate with the severity of disease, as the biological effects and clinical symptoms may depend on which fibril polymorphs are present within amyloid deposits[60].

Although it is fascinating to dissect the effects of different oligomers and fibrils in cellular dysfunction, it is likely that a combination of species will correlate with disease. Amyloid formation is a dynamic process, with monomers and oligomers in rapid exchange with each other[148]. Oligomers can also be generated directly, by loss of monomers and/or oligomers from fibril ends[190,191] (FIG. 2). This phenomenon may be enhanced by the cellular environment, such as the low pH of endosomes and lysosomes[190]. The protein concentration in cells is also finely tuned, with tight coupling of the rates of protein synthesis and degradation to keep proteins within their solubility limit[192,193]. Given this balance, it is perhaps not surprising that overproduction of a protein can trigger wholesale aggregation of susceptible proteins that are at the cusp of their solubility in the cell[194–196]. Precursor mutation, changes in post-translational modifications, stress or ageing can also result in a breakdown of these usually highly protective networks, leading to aggregation.

What emerges from a consideration of this complex network of interactions is the need to elucidate the structures of protein aggregates at atomic resolution. This knowledge would help us to understand how these aggregates perturb cells in molecular detail and to identify methods and molecules that can help control protein aggregation, with beneficial effects on cellular dysfunction and disease. In addition, we also need to explore why assembly of functional amyloid does not result in cell death. Although a number of mechanisms may be employed to prevent toxicity, such as sequestering functional amyloids within membrane-bound compartments[42], the comparison of the structures of functional and disease-associated amyloid fibrils and their assembly mechanisms will be required to reveal how amyloid toxicity can be avoided when fibril assembly is beneficial to the organism.

Diversity of amyloid structures at high resolution

Amyloid fibrils are held together by a large variety of inter-monomer and inter-fibril interactions. The particular modes of interaction vary in different fibril structures formed from the same protein, as well as fibrils formed from different proteins. These interactions affect the physical properties of the fibril assemblies, which may contribute to the phenotypic effects observed for different fibril polymorphs.

Amyloid fibril structure at the subunit level. The defining structural feature of amyloid fibrils is the cross-β fold that all fibrils share. This 'amyloid fold' involves a ladder of stacked β-strands oriented perpendicular to the

Pi-stacking interactions
Attractive, noncovalent interactions between aromatic rings (phenylalanine, Tyr and Trp in proteins).

Biofilm
A group of microorganisms that have adhered to each other and/or a surface.

Gram-positive organisms
Bacteria that possess a peptidoglycan-containing cell wall, which can be positively stained with crystal violet dye, known as Gram stain.

fibril axis, with each 'rung' of the cross-β ladder separated by a 4.7–4.8 Å spacing that arises from the regular hydrogen bond distance between paired carbonyl and amide groups in adjacent β-strands (FIG. 4). This spacing was first demonstrated in 1968–1969 using X-ray fibre diffraction[41,197] (FIG. 1) and is found in all amyloid fibrils irrespective of the sequence of the protein precursor. The presence of the cross-β conformation has now been verified as ubiquitous in amyloid fibrils, whether functional or disease-related, using X-ray fibre diffraction[198], X-ray crystallography[63], cryo-EM[199] and Fourier transform infrared spectroscopy (FTIR)[200]. In FTIR, the strong hydrogen bonds between adjacent β-strands in the cross-β fold absorb at a characteristic frequency of ~1,618 cm^{-1}, whereas the more twisted, less stable β-sheets in globular proteins absorb at longer wavelengths[201,202].

It is important to note that there are several fibrillar structures that are not considered to be amyloid despite sharing some traits. For example, small aromatic molecules (such as diphenylalanine[203]) assemble into fibril-like structures stacked with a 3.4 Å spacing and stabilized by pi-stacking interactions[204]. Because these structures are not composed of protein, they are generally not considered amyloid, despite their structural similarity and the fact that they are also deleterious to cells[204], although there are no reports of disease caused by such 'chemi-fibrils'. Other proteinaceous assemblies have features reminiscent of amyloid but violate some of the defining characteristics of the amyloid fold. For example, short helix–turn–helix peptides assemble into twisted fibrils, stabilized by stacked α-helices[205]. Fibrils in which α-helices, rather than β-strands, orient perpendicular to the fibril axis (so-called cross-α) are also found in vivo, where they are important for biofilm formation in Gram-positive organisms[206]. For example, a toxic oligomer of SOD1, associated with ALS (TABLE 1),

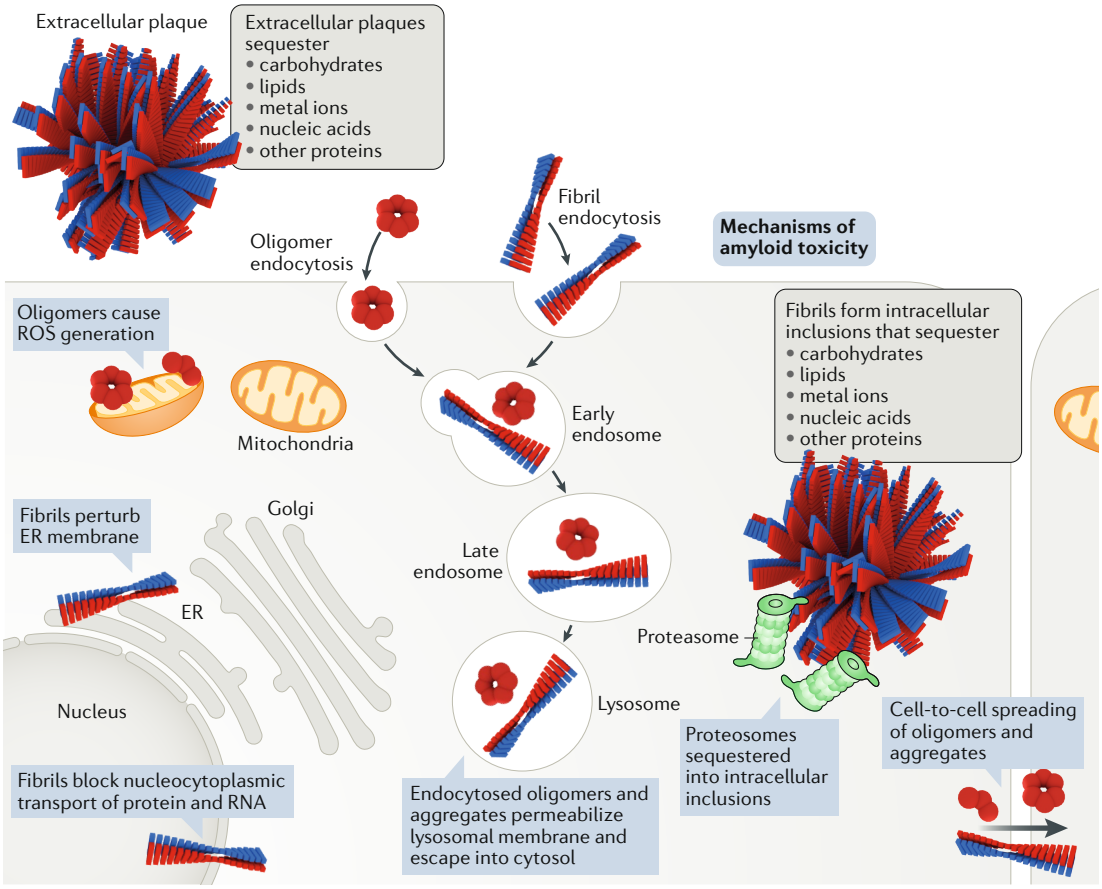

Fig. 3 | **Amyloid aggregates can cause cell disruption by a variety of mechanisms.** Amyloid aggregates can deposit extracellularly or intracellularly, and both can give rise to cellular dysfunction and disease. The aggregates that form from different protein precursors may have different cellular effects, but deconvoluting the toxic mechanism of an individual protein and its ensemble of misfolded or aggregated states (misfolded monomers, oligomers, fibrils or plaques and intracellular inclusions) remains a challenge. Plaques and inclusions sequester a range of other molecules that include glycosaminoglycans[12,188], lipids[158,297] and metal ions[237], which stabilize their assembly. Plaques are physically large and can disrupt organ function by their sheer size. Small fibrils can also be taken up into a cell via endocytosis, but this can be perturbed by preventing binding to certain cell surface receptors such as lymphocyte activation gene 3 protein[267]. Within endosomes and lysosomes, fibrils can release toxic oligomers and can disrupt the endosomal and lysosomal function and dynamics because fibrils are highly resilient to degradation[190,298]. Fibrils can also access the intracellular space following release from cells, thus spreading disease by uptake into adjacent cells. Other effects of aggregates within cells include disruption of endoplasmic reticulum (ER) dynamics[84], release of reactive oxygen species (ROS)[156] from mitochondria and the induction of stress responses[121] (not shown here).

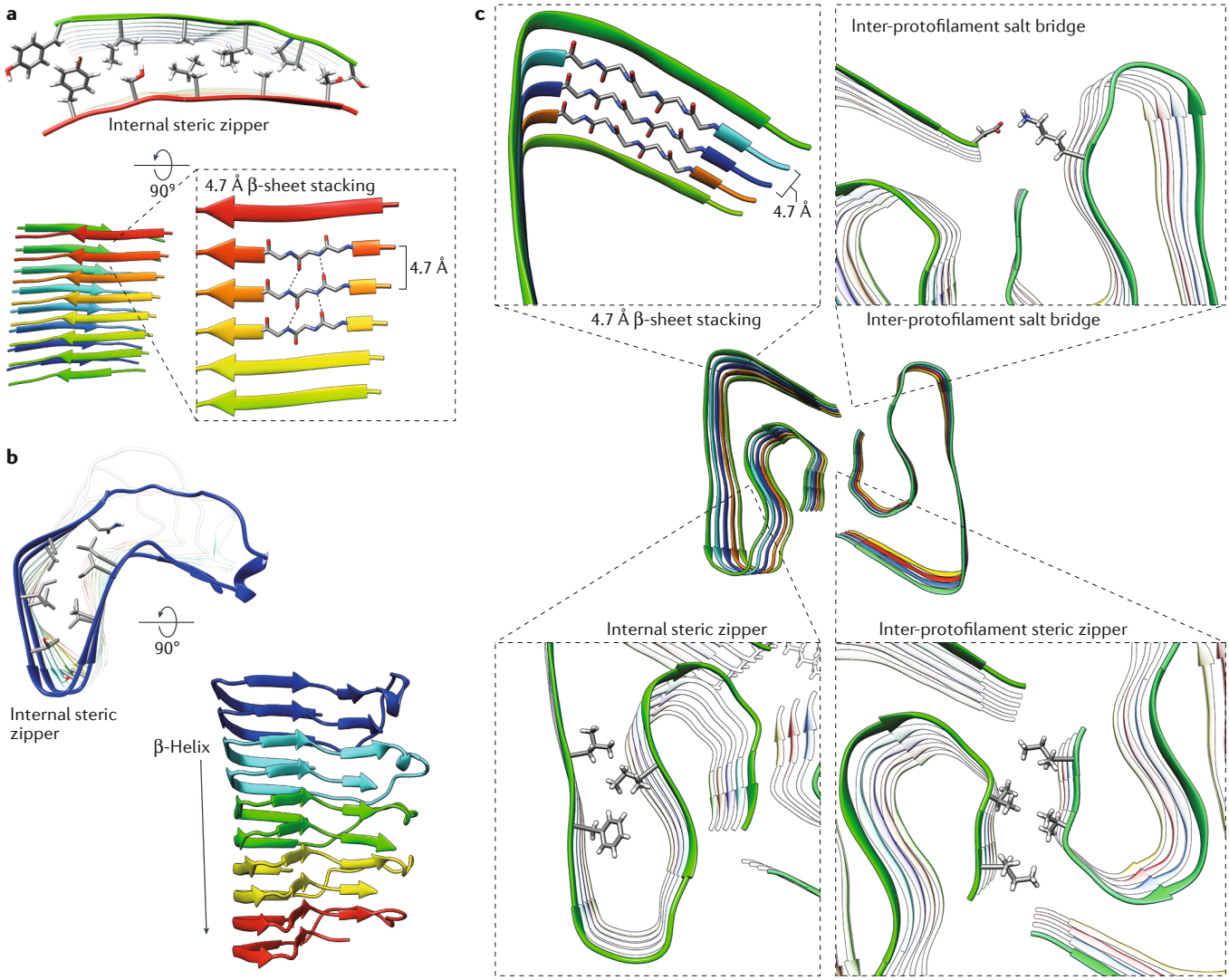

Fig. 4 | **Structural motifs that stabilize amyloid fibrils. a** | A ten-residue peptide from transthyretin (TTR), showing β-sheet stacking in which each β-strand 'rung' is stabilized by hydrogen bonds (denoted by fine black dotted lines) between the polypeptide backbones of precursors, which are separated by the canonical 4.7–4.8 Å repeat of the cross-β amyloid fold (PDB accession number 2nm5 (REF.[67])). Further stabilization is provided by a steric zipper between the β-sheets, which stabilizes the fibril core. **b** | The β-helix of HET-S illustrating its steric zippers (PDB accession number 2rnm (REF.[66])). **c** | A structure of amyloid-β (Aβ)42 fibrils (PDB accession number 5oqv (REF.[27])) illustrating the variety of interactions that stabilize the fibril, including β-strand stacking (top left), formation of inter-protofilament salt bridges (top right), intra-protofilament steric zippers (bottom left) and inter-protofilament steric zippers (bottom right).

shares many structural and pathological characteristics with amyloid but is not considered as a canonical amyloid as its β-sheets are arranged in a corkscrew stack at an ~45° angle to the fibril axis, akin to an extended β-barrel[207]. A similar structure has been observed in an oligomer called cylindrin, assembled from a β-hairpin peptide derived from αβ-crystallin[208]. Interestingly, this cylindrin structure is toxic to HeLa and HEK293 cells[208].

Although the 4.7–4.8 Å stacked β-strand motif is the signature of amyloid, some amyloid fibrils also share features at a larger length scale. Some of the earliest EM observations of fibrils isolated from patient spleens described 'beads' with an ~100 Å periodicity down the fibril axis[209]. Later cryo-EM studies of fibrils formed in vitro from PrP and β_2m reported repeats of ~60 Å (REF.[210]) or 52.5 Å (REF.[211]), respectively, in addition to the canonical ~4.7 Å cross-β repeat, suggestive of higher-order repeating structures. These longer repeats have not been observed in the high-resolution structures of tau or Aβ42 fibrils reported recently[27,28], leaving the structural basis of these larger repeats open to debate.

Other common features are found in the subunit structures of amyloid fibrils regardless of the sequence and structure of their precursor (TABLE 1). In all cases, the subunit structure adopted within the fibril is dramatically different from that of the native protein (TABLE 1). Thus, a major structural conversion must occur as amyloid forms: from unfolded to β-strand, α-helical to β-strand or reorganization of pre-existing β-sheet structures (TABLE 1). Despite the commonality

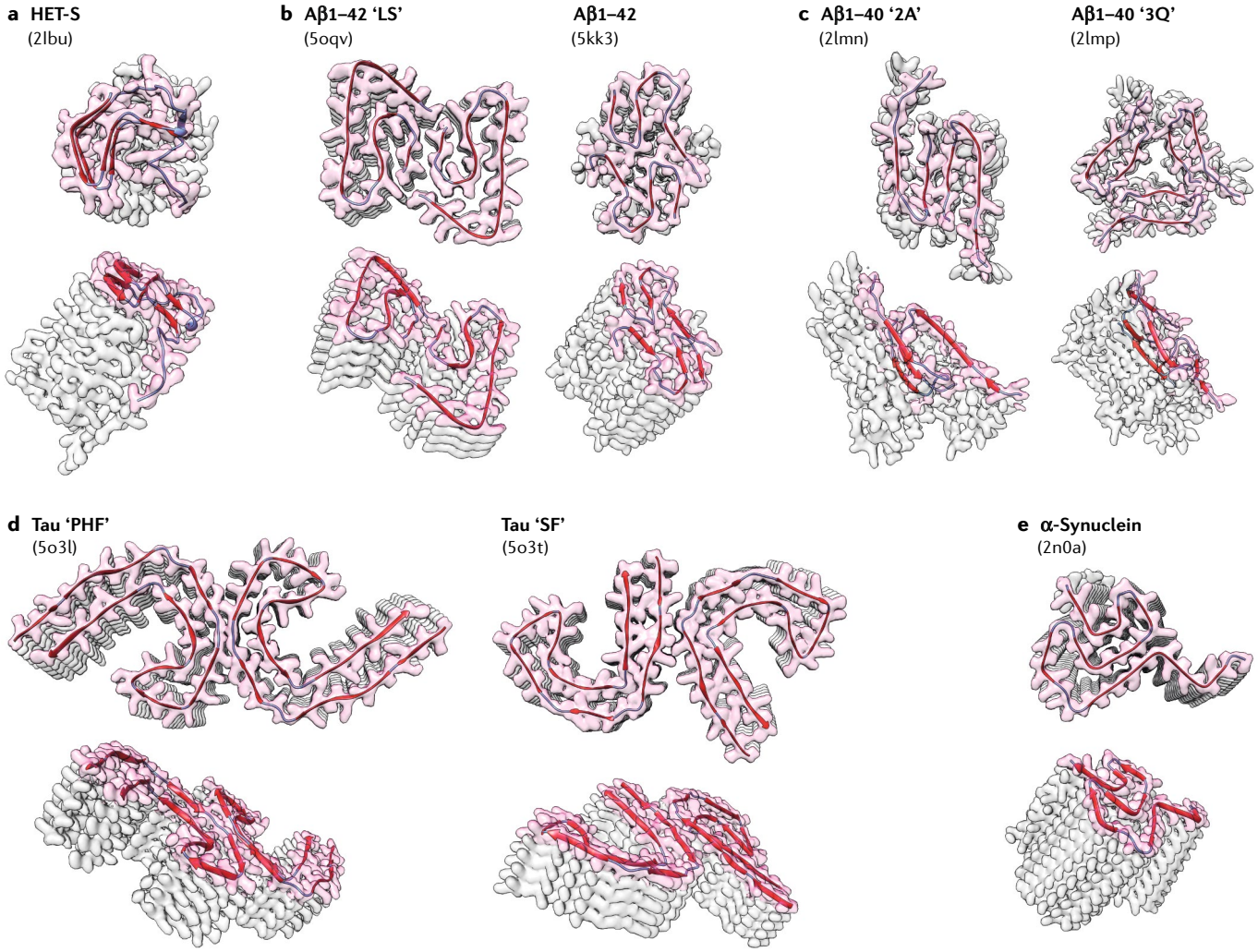

Fig. 5 | **Subunit packing in amyloid fibrils.** Space-filling representations of near-atomic-resolution models of different amyloid fibrils, each filtered to 4 Å. Individual subunits are coloured in red to highlight different inter-protofilament packing in different fibril types. **a** | The β-helix of HET-S that forms a single filament (PDB accession number 2lbu (REF.[66])). **b** | Two polymorphs of amyloid-β (Aβ)42 fibrils formed under different growth conditions (PDB accession number 5oqv[27] (left) and PDB accession number 5kk3 (REF.[278]) (right)). **c** | Two polymorphs of Aβ40. Fibrils formed under the same solution conditions but propagated from seeds with different morphologies (2A, PDB accession number 2lmn (REF.[212]) (left) and 3Q, PDB accession number 2lmp (REF.[212]) (right)). **d** | Two polymorphs of tau fibrils: paired helical (PHF) (left) (PDB accession number 5o3l (REF.[28]) and straight (SF) (right) (PDB accession number 5o3t (REF.[28])). **e** | The single filament of α-synuclein fibrils (PDB accession number 2n0a[216]). The main chain of the top layer of polypeptide chain in each fibril is shown in red. '2A' indicates fibrils with two-fold symmetry; '3Q' indicates fibrils with three-fold symmetry.

of their cross-β fold, fibril structures are not identical, with recent studies revealing a remarkable diversity of architectures that all conform to the amyloid fold (FIG. 5). A ten-residue peptide from TTR[67] forms antiparallel β-strand pairs, with each peptide forming one rung of the cross-β ladder, whereas Aβ40 forms distinct fibril structures that have an in-register parallel organization of their β-strands but differ in the precise location and/or organization of their β-loop β-motif[212,213] (FIG. 5c). In larger proteins, multiple sets of antiparallel β-sheets, termed super-pleated β-sheets, were predicted for a Ure2p prion filament[214] and IAPP fibrils[215], whereas a more complex arrangement in which the β-strands form so-called Leu-Ser motifs that then stack in a parallel in-resister arrangement on the fibril long axis were observed in a structure of a fibril formed by Aβ42 (FIG. 5b, left)[27,65]. Other fibril structures with complex organization of the β-strands within each rung of the cross-β ladder have been observed, including those of α-synuclein[55,216] (FIG. 5e) and tau[28] (FIG. 5d). What is clear is that very different organizations of polypeptide chains can stack into a fibril that conforms to the cross-β structure of amyloid. As more atomic structures of amyloid fibrils are solved, it will be interesting to see just how many different organizations of β-strands will fall under the umbrella of the cross-β fold.

In all of the amyloid fibril structures determined to date with atomic precision, the β-strands are stabilized by dry 'steric zippers'[51] (tight interfaces of interdigitated hydrophobic side chains that exclude water (FIGS 4,5))

and almost perfect packing of their amino acid side chains. These zippers appear to be unique to amyloid fibrils, as they have not yet been observed in a globular protein or in other natural fibrous proteins[51]. Eisenberg's original description of the steric zipper interface was based on structures from microcrystals of short peptides derived from amyloid-forming proteins, including fragments of Aβ, tau, PrP, insulin, IAPP, lysozyme, β_2m and α-synuclein[51]. This work described eight classes of zipper — four formed from parallel β-strands and four from antiparallel β-strands[51]. Five of the eight proposed structures were observed experimentally[51]. Microcrystals have similarities with fibrils in that they can grow under similar conditions, have an ~4.7 Å repeat in their unit cells[217] and, in some cases, small changes in conditions drive interconversion of fibrils into crystals and vice versa[218]. Peptide microcrystals can also seed fibrils of similar morphology from the full-length protein[54], suggesting that steric zippers are the 'core' of amyloid fibrils formed by their intact protein counterparts[54,55]. However, the steric zippers identified in fragments of tau[53] did not form similar zippers in the cryo-EM structure of fibrils formed from the full-length protein[28], although this does not preclude formation of zippers by these regions in tau fibrils with different morphologies.

Proteins with a cross-β structure are also found in β-helices[219,220]. These structures are stabilized by a specific pattern of hydrophilic side chains on the outside of the β-helix and hydrophobic side chains on the inside, along with a terminal glycine[220] (FIG. 4b). β-Helices have been formed from designed peptides[221], are found in soluble proteins (including a variety of bacterial lyases[222], antifreeze proteins[223] and viral tail spikes[224]) and have been implicated in the formation and prionic nature of fibrils in fungi and other organisms[28,198,225]. High-resolution structures of tau fibrils determined using cryo-EM[28] and HET-S from ssNMR[66,226] show β-helix motifs with very similar backbones (root-mean-square deviation (r.m.s.d.) 1.3 Å) despite low sequence similarity in their β-helical regions. Together, the results highlight the array of possible structures that conform to the general amyloid fold but that differ in the details of how their β-strands are arranged.

Filament architecture of the amyloid fibril. The morphology of an amyloid fibril is determined by the number and arrangement of protofilaments that form the fully assembled fibrils[28,64,70–72,211,227] as well as the structure of the subunit itself. Variation in the arrangement and type of interactions between protofilaments adds to the diversity of the amyloid fold. Some amyloid fibrils comprise a single protofilament (for example, the β-helix of HET-S[66] (FIGS 4b,5a)), but the majority contain multiple protofilaments[27,28,64,199,227] that twist together[68,228–230]. Different twists are observed between fibrils formed in the same growth mixture[70,211,229] and even within a single fibril. Other arrangements of protofilaments have been found, including cylinders[231], flat ribbons[64,227,230] and pseudo-crystalline sheets[218]. Protofilaments in twisted fibrils have been found with a variety of symmetries viewed down the fibril axis as well as pairing in an asymmetrical manner[28]. These symmetries include two or three monomeric units in the same plane (in-register two-fold and three-fold)[212,213] and 2_1 screw symmetries[27,28] (a rotation of 180° followed by a translation of half of the β-sheet spacing down the fibril axis). In the recent high-resolution cryo-EM structures of tau and Aβ42, the protofilaments pack in a parallel manner, giving the fibril polarity[27,28]. By contrast, lower-resolution cryo-EM reconstructions of β_2m fibrils suggest that fibrils constructed from both nonpolar (antiparallel) and polar (parallel) arrangements of protofilaments are formed within the same preparation[211]. However, it should be noted that no high-resolution structure of a nonpolar fibril with an antiparallel arrangement of its protofilaments has yet been determined. Mass per unit length (MPL) measurements using scanning transmission EM (STEM)[65,211,227] have been used to determine the number of protofilaments in β_2m[211], IAPP[228] and α-synuclein[216] fibrils and to differentiate polymorphs of Aβ40 with two-fold and three-fold symmetry structures[58,212,213,232] (FIG. 5c). MPL can also be determined by tilt-beam transmission EM (TB-TEM) imaging[233] or by mass spectrometry of whole fibrils[234], although STEM remains the most commonly used approach.

The arrangements of the protofilaments in recently determined amyloid fibril structures are shown in FIG. 5. These include the 2A and 3Q fibrils of Aβ40 described above (FIG. 5c), in which different fibril morphologies correspond to different organization of similar (but not identical) β-loop–β subunit motifs[212]. In other cases, including the paired helical and straight filaments of tau[28], different fibril morphologies are formed by identical subunits held together by different interactions (FIG. 5d). Although the cryo-EM structures of the tau polymorphs provide the first direct evidence for different fibril morphologies arising from alternative packing of identical subunits, this phenomenon has been suggested for α-synuclein[64,230], Aβ40 (REFS[71,72]), TTR[67] and β_2m[211] fibrils. Protofilaments in paired helical filaments of tau[28] are stabilized by backbone hydrogen-bonding within its $_{332}$PGGGQ$_{336}$ sequence, which forms an antiparallel poly-glycine (polyG) II β-spiral[235], as well as by hydrogen bonding between the side chain of Gln336 and the backbone of Pro332 in the opposing protofilament. In the recent cryo-EM structure of Aβ42 (REF.[27]), the protofilaments were shown to be held together by a hydrophobic steric zipper involving the Val39 and Ile41 side chains from each protofilament and stabilized further by a salt bridge between the amino-terminal Asp and Lys28 side chains of opposing protofilaments (FIG. 4c). By contrast, in the asymmetrical straight filament (SF) tau polymorph[28], neither backbone nor side chain interactions between protofilaments appear to play a large role in stabilizing its structure. Instead, six side chains (Lys317, Lys321 and Thr319 from each protofilament) coordinate an unknown density that the authors predict is the amino-terminal $_7$EFE$_9$ of each tau subunit. This density could, however, involve another polyanionic molecule such as a glycosaminoglycan or nucleic acid in this crude brain extract[28]. Analyses of amyloid fibrils of α-synuclein with stripes of high electron density running down the fibril axis[230,236] suggest a role for metal ions in stabilizing fibrils, consistent with many studies

that have proposed metal ion binding in the initiation of amyloid formation[237].

Data from X-ray diffraction and micro-ED[52] of small, amyloidogenic peptides have been used to predict the formation of steric zippers[53–55,76]. As the crystal packing interactions in these steric zippers are necessarily formed between identical peptides, they can predict only regions that self-associate in symmetrical, paired protofilaments. A structure of the NAC core domain of α-synuclein by micro-ED[55] was interpreted as showing possible candidates for inter-protofilament steric zippers in fibrils formed from the intact 140-residue protein. Despite identification of several polymorphs of α-synuclein fibrils composed of twisted protofilaments[227,230], as yet no high-resolution structure of α-synuclein fibrils containing multiple protofilaments is available to validate this hypothesis.

The recent structures of amyloid fibrils show that the same primary sequence can assemble into different structures, even under the same growth conditions[76,187,238,239]. This finding is in stark contrast with the folding of the vast majority of globular proteins, in which a given sequence forms the same fold every time it emerges from the ribosome or is folded in vitro[240]. Moreover, amyloid formation is slow, despite being thermodynamically favoured; therefore, it can take an extraordinarily long time, possibly years in vitro[241], for fibril growth to reach equilibrium. Thus, the morphology of fibrils can change over time[241] and in response to changing environmental conditions[77]. In energetic terms, the energy landscape of fibril formation is far more rugged and complex than that for globular proteins, potentially involving multiple intermediates, parallel assembly pathways and resulting in diverse amyloid end products with different cross-β structures[242].

Amyloid polymorphism in disease

How the observed structural polymorphism of amyloid fibrils affects disease onset, progression and presentation is not well understood. What is clear is that variations in the precursor protein's gene sequence can be directly tied to variation in both the age of onset and disease duration in numerous amyloid diseases (FIG. 6).

Although the development of disease can take place over different timescales in individuals affected by polyQ expansion diseases, AD and PD (FIG. 6), in prion diseases death is observed over an extraordinarily narrow window of a few days[243]. Humans also show extended incubation periods in CJD[244] but have short disease duration (typically 6 months), which is thus far unique to these diseases. In contrast to prion disorders, mouse models of AD result in death over a much wider time span[245], as is observed in humans[60], although the ability for mouse models to accurately recapitulate disease processes in humans is debated[245]. In Huntington disease, individuals containing huntingtin with fewer than 35 Gln residues appear healthy over their lifetime. However, individuals with longer polyQ repeat lengths show an age of onset and severity of disease that correlates with the number of Gln residues above this critical threshold[105] (FIG. 6, top left). In Machado–Joseph disease, another polyQ disorder in which ataxin 3 contains a glutamine expansion, the non-pathological polyQ repeat length is 12–40 residues, with pathology not presenting until 62 repeats[105]. The wide range in the number of repeats, coupled with the fact that increasing the number of repeats increases the severity of disease symptoms, suggests that polymorphic effects due to primary sequence expansion are linked with disease[105].

PD can be caused by mutations within the *SNCA* gene, which encodes α-synuclein, with variants such as A30P, E46K, H50Q, G51D and A53T leading to early-onset disease and shorter disease duration[102,246–249] (FIG. 6, lower left). For example, the G51D variant is as aggressive as quadruplication of the *SNCA* gene in terms of age of disease onset but has also been shown to induce other symptoms, including epilepsy[250]. Although gene multiplication decreases the age of onset of PD, as expected from an increased concentration of the precursor protein, the additional symptoms in patients with *SNCA* gene multiplications cannot be accounted for simply by amyloid load. This finding adds weight to the view that specific amyloid polymorphs may explain the observed phenotypes of PD[250]. Specific point mutations can give rise to diverse effects on cognitive impairment, psychiatric disturbances, hallucinations, autonomic dysfunction and the previously mentioned symptoms[250].

Primary sequence variations including sequence expansions (such as polyQ, polyA and poly-GlyAla expansions[93]) or single point mutations (such as those described for α-synuclein above) may result in a different subunit fold and subunit packing in the fibril. Consistent with this notion, ssNMR studies of fibrils formed from the 'Osaka' (ΔE22) and 'Iowa' (D23N) mutants of Aβ40 revealed structures that are different from those formed by wild-type Aβ40/42 (REFS[61,251]). Links between polymorphism and pathology in fibrils with identical primary sequences are less clear but still evident. The age of disease onset in patients with Huntington disease has been correlated with the number of CAG repeats[252], and different polymorphs of Aβ40 (REF.[253]) and α-synuclein[227] have both different cytotoxicity in vitro and different rates of plaque deposition in vivo on the basis of the source of the fibrillar seed material[254,255]. Different cytotoxicity was also observed in fibrils of full-length IAPP seeded from toxic and non-toxic short peptide fibrils[54]. Isolation and characterization of fibrils from patients also suggest that fibril morphology varies from patient to patient. As discussed above, seeding fibril formation of Aβ40/42 using plaques extracted from patients who displayed different disease phenotype and progression resulted in different ssNMR spectra[60,213], suggesting that a different fibril polymorph was predominant in each patient. This is not to suggest that all fibrils formed in vivo will be monomorphic. Indeed, multiple polymorphs of tau were present in a single patient-derived sample[28], and various Aβ polymorphs have been identified within the same patients using X-ray diffraction[256]. Further evidence comes from analysis of fibrils seeded from ex vivo material from patients who presented either the posterior cortical atrophy form of AD (PCA-AD), rapid-AD (r-AD) or typical AD (t-AD)[60]. A single Aβ40 polymorph was most abundant in PCA-AD and t-AD,

Polymorphism
The same protein can assemble into amyloid fibrils that have different arrangements of subunits in the fibril, numbers of protofilaments, widths and/or crossover distances.

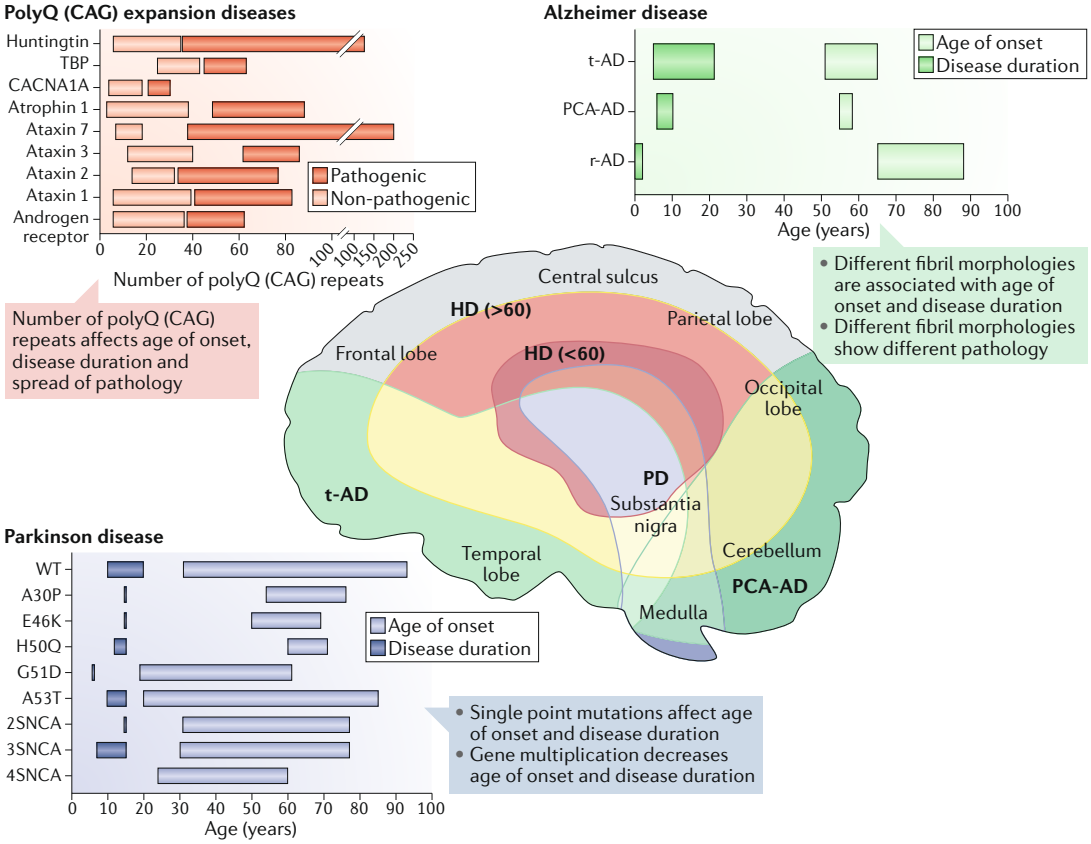

Fig. 6 | **How changes in primary sequence affect amyloid disease.** Top left panel: various diseases are caused by poly-glutamine (polyQ) expansion disorders. Depending on the specific disease (shown in the figure), polyQ repeat lengths exceeding a critical threshold can cause disease, whereas fewer repeats are innocuous. Data were taken from REFS[93,105]. Lower left panel: the age of onset of patients with Parkinson disease (PD) is influenced by the copy number of the α-synuclein gene (duplication (2SNCA), triplication (3SNCA) or quadruplication (4SNCA)), with increased expression correlating with earlier onset. Age of onset and disease duration are also influenced by single point mutations, which may result in different aggregation pathways and/or kinetics or different fibril architectures resulting in different disease phenotypes. Data were taken from REFS[299,300]. Top right panel: the pathology of Alzheimer disease (AD) can be influenced by fibril morphology. In particular, typical-AD (t-AD) and a rapidly progressive form of AD (r-AD) show similar fibril architecture monitored by solid-state NMR spectroscopy (ssNMR) but have varied ages of onset and disease duration. However, in posterior cortical atrophy AD (PCA-AD), fibrils with a different structure are formed. The age of onset and disease duration for PCA-AD are similar to t-AD and r-AD, but the disease primarily affects the cerebellum rather than the temporal lobe. Centre panel: a diagram of the brain highlighting the regions primarily affected by each of the diseases shown. CACNA1A, voltage-dependent P/Q-type calcium channel subunit α1A; HD, Huntington disease; TBP, TATA-box-binding protein; WT, wild type. The top right panel was adapted from REF.[60].

whereas the r-AD samples contained a higher proportion of additional structures. Again, the ex vivo samples were structurally distinct from synthetic strains created in vitro, highlighting remarkable strain polymorphism even within an individual patient[60].

The diversity of amyloid polymorphs could explain the different disease phenotypes observed in patients in which the same APP aggregates. Alternatively, given that fibril formation can take years to reach equilibrium[241], fibrils may slowly change in structure. Indeed, fibril plaques of Aβ in transgenic mouse models have been shown to undergo structural rearrangement[257], and different α-synuclein fibril polymorphs evolve over time in vitro[241]. Fibril structures in patients may thus vary during disease progression. Such findings may explain why amyloid plaque load does not correlate with disease symptoms[258,259]; thus, confirmation of fibril structure post-mortem is needed to link fibril structure with disease type.

Potential for therapeutic interventions

Studies into which amyloid structure is associated with a particular presentation of disease are in their infancy, but development of better diagnostics may help to identify patients in most need of urgent therapeutic intervention. Disease is currently diagnosed using cerebral spinal fluid diagnostics, positron emission tomography (PET) imaging and detection of oligomers using immunoassays, including conformation-dependent approaches[260]. However, personalized amyloid-blocking medicines tailored to the specific amyloid polymorphs present in individual patients remain an aspiration. At present, with one notable exception[261], no therapeutics have been shown to reduce amyloid formation in humans.

Another important consideration in targeting these devastating diseases is when in the amyloid aggregation cascade or disease process to intervene. This consideration is exacerbated by the dynamic nature of the precursors of amyloid formation that are unfolded, non-native or partially folded, precluding structure-based drug design. Decreasing the concentration of monomer would reduce the total amount of protein available to form amyloid, but such strategies could be deleterious if the monomer has a vital functional role. Interestingly, however, the function of several amyloid proteins remains unresolved[262,263]. Perturbing oligomer formation (FIG. 2) may offer a route to treatment, but the dynamic nature of these species makes them difficult to target[264], and no high-resolution amyloid oligomer structures are currently available to guide such efforts. Decreasing the population of any one oligomer may drive the equilibrium towards a more toxic assembly. Small molecules could be sought to prevent oligomer formation or, conversely, to promote fibrillation, which, in turn, would decrease the lifetime and hence toxic potential of the oligomeric species. Designing interventions that promote the assembly of less toxic fibril polymorphs might also reduce disease severity.

Another approach would be to promote the sequestration of amyloidogenic monomers into non-amyloid amorphous aggregates[265], although this could itself have deleterious effects. Finally, preventing the spread of toxic species may offer a new form of intervention. Oligomers have been shown to interact with many cellular surface receptors in both presynaptic and postsynaptic membranes, such as ephrin-type B receptor 2 (EphB2), PrP^C (REF.[266]), renal tumour antigen (RAGE; also known as MOK) and scavenger receptor class A (SCARA) and class B (SCARB), mediating both their toxic effects and internalization. Other cell surface receptors such as lymphocyte activation gene 3 protein (LAG3) (REF.[267]) have been shown to be important for endocytic import of fibrillar species. Containing toxic species in individually affected cells and/or preventing uptake by antibody blocking of receptors[267] may prevent the prion-like spread and hence may halt the progression of disease. Knowing where to intervene relies on identifying the toxic species in amyloid aggregation, which may depend on the protein sequence and/or the cell types involved. Culprits could include any or all of on-pathway and off-pathway oligomers as well as the fibrils themselves[268].

Although effective therapy still currently remains out of reach, both drug-dependent and drug-resistant strains of prion diseases have been reported[269–271], suggesting that an opportunity for therapeutic intervention does exist. Moreover, small molecules, peptides and peptidomimetics able to target different, but closely related, steric zippers have been successfully designed[272–274], giving hope that we will soon be able to identify which amyloid fibrils form in different individuals and hence to relate amyloid structure and assembly to disease type and aetiology. What is needed at the current time is the ability of reagents able to stabilize oligomers with specific conformations or to prevent their formation so that the link between disease and the population of a specific conformeric species can be defined for different amyloid diseases. In a similar vein, reagents able to guide amyloid formation to a specific, well-defined structural state will also enable the link between fibril formation and disease to be made. What is clear is that the answer may be different for different proteins and protein sequences; hence, an understanding of amyloid structure and of oligomer structure and conformation is going to be required before the key question of what causes amyloid disease can be answered at last.

Conclusions and future perspectives

Amyloid fibrils have highly organized hierarchical structures that are built from protofilaments in which individual monomeric subunits form (most often) parallel in-register β-strands. These protofilaments then pack against each other, forming fibrils that are stabilized by dry steric interfaces. Further inter-fibril interaction leads to the formation of the plaques and inclusions characteristic of amyloid disease. Recent advances in cryo-EM and ssNMR have given insights into the structure of amyloid fibrils in unprecedented detail, revealing a variety of structures that conform to the cross-β amyloid fold. Coupling these techniques with orthogonal data (for example, with other biophysical measurements) and data on disease type, presentation and progression will help to elucidate which amyloid formation pathways, amyloid intermediates and/or fibril structures are responsible for disease. As the capabilities of cryo-ET improve, we will be able to study amyloid fibrils and plaques and intracellular inclusions in situ with increased resolution. This increased resolution will allow us to discern how polymorphism relates to disease phenotype and how fibril structure affects and is affected by the cellular environment. The time has never been better to finally understand amyloid structure, protein aggregation mechanisms and how they relate to disease. In turn, these breakthroughs bring new hope and renewed vigour in our quest to develop agents that can diagnose, delay or even halt the progression of disease.

Published online: 20 September 2018

1. Sipe, J. D. & Cohen, A. S. Review: History of the amyloid fibril. *J. Struct. Biol.* **130**, 88–98 (2000).
2. Goedert, M., Wischik, C. M., Crowther, R. A., Walker, J. E. & Klug, A. Cloning and sequencing of the cDNA encoding a core protein of the paired helical filament of Alzheimer disease: identification as the microtubule-associated protein tau. *Proc. Natl Acad. Sci. USA* **85**, 4051–4055 (1988).
3. Murphy, M. P. & LeVine, I. I. I. H. Alzheimer's disease and the β-amyloid peptide. *J. Alzheimers Dis.* **19**, 311–323 (2010).
4. Stefanis, L. α-Synuclein in Parkinson's disease. *Cold Spring Harb. Perspect. Med.* **2**, a009399 (2012).
5. Protein Data Bank. Yearly growth of total structures. *rcbs.org* http://www.rcsb.org/pdb/statistics/contentGrowthChart.do?content=total (2018).
6. Sipe, J. D. et al. Amyloid fibril proteins and amyloidosis: chemical identification and clinical classification international society of amyloidosis 2016 nomenclature guidelines. *Amyloid* **23**, 209–213 (2016).
7. Sloane, P. D. et al. The public health impact of Alzheimer's disease, 2000–2050: potential implication of treatment advances. *Annu. Rev. Publ. Health* **23**, 213–231 (2002).
8. Geula, C. et al. Aging renders the brain vulnerable to amyloid beta-protein neurotoxicity. *Nat. Med.* **7**, 827–831 (1998).
9. Woerner, A. C. et al. Cytoplasmic protein aggregates interfere with nucleocytoplasmic transport of protein and RNA. *Science* **350**, 173–176 (2016).
10. Guo, Q. et al. In situ structure of neuronal C9orf72 poly-GA aggregates reveals proteasome recruitment. *Cell* **172**, 696–705 (2018).

11. Drummond, E. et al. Proteomic differences in amyloid plaques in rapidly progressive and sporadic Alzheimer's disease. *Acta Neuropathol.* **133**, 933–954 (2017).
12. Stewart, K. L. et al. Atomic details of the interactions of glycosaminoglycans with amyloid-β fibrils. *J. Am. Chem. Soc.* **138**, 8328–8331 (2016).
13. Kollmer, M. et al. Electron tomography reveals the fibril structure and lipid interactions in amyloid deposits. *Proc. Natl Acad. Sci. USA* **113**, 5604–5609 (2016).
14. Knowles, T. P. J. et al. Role of intermolecular forces in defining material properties of protein nanofibrils. *Science* **318**, 1900–1903 (2007).
15. Smith, J. F., Knowles, T. P. J., Dobson, C. M., MacPhee, C. E. & Welland, M. E. Characterization of the nanoscale properties of individual amyloid fibrils. *Proc. Natl Acad. Sci. USA* **103**, 15806–15811 (2006).
16. Greenwald, J., Friedmann, M. P. & Riek, R. Amyloid aggregates arise from amino acid condensations under prebiotic conditions. *Angew. Chem. Int. Ed. Engl.* **55**, 11609–11613 (2016).
17. Romero, D., Aguilar, C., Losick, R. & Kolter, R. Amyloid fibers provide structural integrity to *Bacillus subtilis* biofilms. *Proc. Natl Acad. Sci. USA* **107**, 2230–2234 (2010).
18. Taglialegna, A. et al. Staphylococcal Bap proteins build amyloid scaffold biofilm matrices in response to environmental signals. *PLOS Pathog.* **12**, e1005711 (2016).
19. Lipke, P. N., Klotz, S. A., Dufrene, Y. F., Jackson, D. N. & Garcia-Sherman, M. C. Amyloid-like β-aggregates as force-sensitive switches in fungal biofilms and infections. *Microbiol. Mol. Biol. Rev.* **82**, e00035–17 (2018).
20. Garvey, M., Ecroyd, H., Ray, N. J., Gerrard, J. A. & Carver, J. A. Functional amyloid protection in the eye lens: retention of alpha-crystallin molecular chaperone activity after modification into amyloid fibrils. *Biomolecules* **7**, E67 (2017).
21. Biesecker, S. G., Nicastro, L. K., Wilson, R. P. & Tukel, C. The functional amyloid curli protects *Escherichia coli* against complement-mediated bactericidal activity. *Biomolecules* **8**, E5 (2018).
22. Bajakian, T. H. et al. Metal binding properties of the N-terminus of the functional amyloid Orb2. *Biomolecules* **7**, E57 (2017).
23. Audas, T. E. et al. Adaptation to stressors by systemic protein amyloidogenesis. *Dev. Cell* **39**, 155–168 (2016).
24. Guyonnet, B., Egge, N. & Cornwall, G. A. Functional amyloids in the mouse sperm acrosome. *Mol. Cell. Biol.* **34**, 2624–2634 (2014).
25. Fowler, D. M. et al. Functional amyloid formation within mammalian tissue. *PLOS Biol.* **4**, e6 (2006).
26. Roan, N. R. et al. Peptides released by physiological cleavage of semen coagulum proteins form amyloids that enhance HIV infection. *Cell Host Microbe* **10**, 541–550 (2011).
27. Gremer, L. et al. Fibril structure of amyloid-β(1–42) by cryo-electron microscopy. *Science* **358**, 116–119 (2017).
28. Fitzpatrick, A. W. P. et al. Cryo-EM structures of tau filaments from Alzheimer's disease. *Nature* **547**, 185–190 (2017).
29. US National Library of Medicine. *ClinicalTrials.gov* https://www.clinicaltrials.gov/ct2/show/NCT02760602 (2018).
30. US National Library of Medicine. *ClinicalTrials.gov* https://www.clinicaltrials.gov/ct2/show/NCT00606476 (2018).
31. US National Library of Medicine. *ClinicalTrials.gov* https://www.clinicaltrials.gov/ct2/show/NCT01739348 (2018).
32. US National Library of Medicine. *ClinicalTrials.gov* https://www.clinicaltrials.gov/ct2/show/NCT00531804 (2018).
33. Virchow, R. Zur cellulose. *Archiv. Pathol. Anat.* **6**, 416–426 (1854).
34. Friedreich, N. & Kekulé, A. Zur amyloidfrage. *Virchows Arch.* **16**, 50–65 (1859).
35. Puchtler, H., Sweat, F. & Levine, M. On the binding of Congo red by amyloid. *J. Histochem. Cytochem.* **10**, 355–364 (1962).
36. Benditt, E. P., Eriksen, N., Hermodson, M. A. & Ericsson, L. H. The major proteins of human and monkey amyloid substance: common properties including unusual N-terminal amino acid sequences. *FEBS Lett.* **19**, 169–173 (1971).
37. Glenner, G. G., Eanes, E. D., Bladen, H. A., Terry, W. & Page, D. L. Creation of "amyloid" fibrils from Bence Jones proteins in vitro. *Science* **174**, 712–714 (1971).
38. Costa, P. P., Figueria, A. S. & Bravo, F. R. Amyloid fibril protein related to prealbumin in familial amyloidotic polyneuropathy. *Proc. Natl Acad. Sci. USA* **75**, 4499–4503 (1978).
39. Astbury, W. T. & Street, A. X-ray studies of the structure of hair, wool and related fibres. I. General. *Phil. Trans. R. Soc.* **230**, 75–101 (1932).
40. Hall, K. T. *The Man in the Monkeynut Coat* (Oxford Univ. Press, Oxford, 2014).
41. Geddes, A. J., Parker, K. D., Atkins, E. D. T. & Beighton, E. "Cross-β" conformation in proteins. *J. Mol. Biol.* **32**, 343–358 (1968).
42. Jackson, M. & Hewitt, E. Why are functional amyloids non-toxic in humans? *Biomolecules* **7**, E71–E73 (2017).
43. Hewetson, A. et al. Functional amyloids in reproduction. *Biomolecules* **7**, E46 (2017).
44. Ramsook, C. B. et al. Yeast cell adhesion molecules have functional amyloid-forming sequences. *Eukaryot. Cell* **9**, 393–404 (2010).
45. Romero, D. & Kolter, R. Functional amyloids in bacteria. *Int. Microbiol.* **17**, 65–73 (2014).
46. Pham, C. L., Kwan, A. H. & Sunde, M. Functional amyloid: widespread in Nature, diverse in purpose. *Essays Biochem.* **56**, 207–219 (2014).
47. Fowler, D. M., Koulov, A. V., Balch, W. E. & Kelly, J. W. Functional amyloid — from bacteria to humans. *Trends Biochem. Sci.* **32**, 217–224 (2007).
48. Morris, K. L. & Serpell, L. C. *X-Ray Fibre Diffraction Studies of Amyloid Fibrils* (Humana Press, 2012).
49. Eanes, E. D. & Glenner, G. G. X-ray diffraction studies on amyloid filaments. *J. Histochem. Cytochem.* **10**, 673–677 (1968).
50. Kirschner, D. A., Abraham, C. & Selkoe, D. J. X-ray diffraction from intraneuronal paired helical filaments and extraneuronal amyloid fibers in Alzheimer disease indicates cross-beta conformation. *Proc. Natl Acad. Sci. USA* **83**, 503–507 (1986).
51. Sawaya, M. R. et al. Atomic structures of amyloid cross-β spines reveal varied steric zippers. *Nature* **447**, 453–457 (2007).
52. Shi, D., Nannenga, B. L., Iadanza, M. G. & Gonen, T. Three-dimensional electron crystallography of protein microcrystals. *eLife* **2**, e01345 (2013).
53. de la Cruz, M. J. et al. Atomic-resolution structures from fragmented protein crystals with the cryoEM method MicroED. *Nat. Med.* **14**, 399–402 (2017).
54. Krotee, P. et al. Atomic structures of fibrillar segments of hIAPP suggest tightly mated beta-sheets are important for cytotoxicity. *eLife* **6**, e19273 (2017).
55. Rodriguez, J. A. et al. Structure of the toxic core of alpha-synuclein from invisible crystals. *Nature* **525**, 486–490 (2015).
56. Sawaya, M. R. et al. Ab initio structure determination from prion nanocrystals at atomic resolution by MicroED. *Proc. Natl Acad. Sci. USA* **113**, 11232–11236 (2016).
57. Colvin, M. T. et al. High resolution structural characterization of Aβ42 amyloid fibrils by magic angle spinning NMR. *J. Am. Chem. Soc.* **137**, 7509–7518 (2015).
58. Antzutkin, O. N., Leapman, R. D., Balbach, J. J. & Tycko, R. Supramolecular structural constraints on Alzheimer's β-amyloid fibrils from electron microscopy and solid-state nuclear magnetic resonance. *Biochemistry* **41**, 15436–15450 (2002).
59. Chan, J. C. C., Oyler, N. A., Yau, W. & Tycko, R. Parallel β -sheets and polar zippers in amyloid fibrils formed by residues 10–39 of the yeast prion protein Ure2p. *Biochemistry* **44**, 10669–10680 (2005).
60. Qiang, W., Yau, W. M., Lu, J. X., Collinge, J. & Tycko, R. Structural variation in amyloid-beta fibrils from Alzheimer's disease clinical subtypes. *Nature* **541**, 217–221 (2017).
61. Qiang, W., Yau, W. M., Luo, Y., Mattson, M. P. & Tycko, R. Antiparallel beta-sheet architecture in Iowa-mutant beta-amyloid fibrils. *Proc. Natl Acad. Sci. USA* **109**, 4443–4448 (2012).
62. Lührs, T. et al. 3D structure of Alzheimer's amyloid-B(1–42) fibrils. *Proc. Natl Acad. Sci. USA* **102**, 17342–17347 (2005).
63. Nelson, R. et al. Structure of the cross-β spine of amyloid-like fibrils. *Nature* **435**, 773–778 (2005).
64. Vilar, M. et al. The fold of α-synuclein fibrils. *Proc. Natl Acad. Sci. USA* **105**, 8637–8642 (2008).
65. Walti, M. A. et al. Atomic-resolution structure of a disease-relevant Abeta(1–42) amyloid fibril. *Proc. Natl Acad. Sci. USA* **113**, E4976–E4984 (2016).
66. Wasmer, C. et al. Amyloid fibrils of the HET-s(218–289) prion from a β solenoid with a triangular hydrophobic core. *Science* **319**, 1523–1526 (2008).
67. Fitzpatrick, A. W. P. et al. Atomic structure and hierarchical assembly of a cross-β amyloid fibril. *Proc. Natl Acad. Sci. USA* **110**, 5468–5473 (2013).
68. Jiménez, J. et al. Cryo-electron microscopy structure of an SH3 amyloid fibril and model of the molecular packing. *EMBO J.* **18**, 815–821 (1999).
69. Saibil, H. R. et al. Heritable yeast prions have a highly organized three-dimensional architecture with interfiber structures. *Proc. Natl Acad. Sci. USA* **109**, 14906–14911 (2012).
70. Fändrich, M., Meinhardt, J. & Grigorieff, N. Structural polymorphism of Alzheimer Aβ and other amyloid fibrils. *Prion* **3**, 89–93 (2009).
71. Sachse, C., Fändrich, M. & Grigorieff, N. Paired β-sheet structure of an Aβ(1–40) amyloid fibril revealed by electron microscopy. *Proc. Natl Acad. Sci. USA* **105**, 7462–7466 (2008).
72. Sachse, C. et al. Quaternary structure of a mature amyloid fibril from Alzheimer's Abeta(1–40) peptide. *J. Mol. Biol.* **362**, 347–354 (2006).
73. Kirschner, D. A. et al. In vitro amyloid fibril formation by synthetic peptides corresponding to the amino terminus of apoSAA isoforms from amyloid-susceptible and amyloid-resistant mice. *J. Struct. Biol.* **124**, 88–98 (1998).
74. Castaño, E. M. et al. In vitro formation of amyloid fibrils from two synthetic peptides of different lengths homologous to Alzheimer's disease β-protein. *Biochem. Biophys. Res. Commun.* **141**, 782–789 (1986).
75. Aggeli, A. et al. Responsive gels formed by the spontanious self-assembly of peptides into polymeric β-sheet tapes. *Nature* **386**, 259–262 (1997).
76. Colletier, J. P. et al. Molecular basis for amyloid-beta polymorphism. *Proc. Natl Acad. Sci. USA* **108**, 16938–16943 (2011).
77. Gosal, W. S. et al. Competing pathways determine fibril morphology in the self-assembly of beta2-microglobulin into amyloid. *J. Mol. Biol.* **351**, 850–864 (2005).
78. Booth, D. et al. Instability, unfolding and aggregation of human lysozyme variants underlying amyloid fibrillogenesis. *Nature* **385**, 797–793 (1997).
79. Hecht, M. H., Das, A., Go, A., Bradley, L. H. & Wei, Y. De novo proteins from designed combinatorial libraries. *Protein. Sci.* **13**, 1711–1723 (2004).
80. Kühlbrandt, W. The resolution revolution. *Science* **343**, 1443–1444 (2014).
81. Pinotsi, D. et al. Direct observation of heterogeneous amyloid fibril growth kinetics via two-color super-resolution microscopy. *Nano. Lett.* **14**, 339–345 (2014).
82. Kaminski Schierle, G. S. et al. In situ measurements of the formation and morphology of intracellular beta-amyloid fibrils by super-resolution fluorescence imaging. *J. Am. Chem. Soc.* **133**, 12902–12905 (2011).
83. Han, S. et al. Amyloid plaque structure and cell surface interactions of beta-amyloid fibrils revealed by electron tomography. *Sci. Rep.* **7**, 43577 (2017).
84. Bauerlein, F. J. B. et al. In situ architecture and cellular interactions of polyQ inclusions. *Cell* **171**, 179–187 (2017).
85. Tang, M., Comellas, G. & Rienstra, C. M. Advanced solid-state NMR approaches for structure determination of membrane proteins and amyloid fibrils. *Acc. Chem. Res.* **46**, 2080–2088 (2013).
86. Alzheimer, A. Über einen eigenartigen schweren Erkrankungsprozeβ der Hirnrincle. *Neurol. Central* **25**, 1134 (1906).
87. Alzheimer, A. Über eine eigenartige Erkrankung der Hirnrinde. *Allg. Z. Psychiatr. Psych.-Gerichtl. Med.* **641**, 46–48 (1907).
88. Chiti, F. & Dobson, C. M. Protein misfolding, functional amyloid, and human disease: a summary of progress over the last decade. *Annu. Rev. Biochem.* **86**, 27–68 (2006).
89. Eisenberg, D. & Jucker, M. The amyloid state of proteins in human diseases. *Cell* **148**, 1188–1203 (2012).
90. Westermark, P. et al. Amyloid: toward terminology clarification. Report from the Nomenclature Committee of the International Society of Amyloidosis. *Amyloid* **12**, 1–4 (2005).
91. Vassar, R., Bennett, B. D., Babu-Khan, S. & Kahn, S. β-Secretase cleavage of Alzheimer's amyloid precursor protein by the transmembrane aspartic protease BACE. *Science* **286**, 735–741 (1999).
92. Prusiner, S. B., Bowman, K. A., Bendheim, P. E. & Glenner, G. G. Scrapie prions aggregate to form amyloid-like birefringent rods. *Cell* **35**, 349–358 (1983).
93. Warby, S. C. et al. CAG expansion in the Huntington disease gene is associated with a specific and targetable predisposing haplogroup. *Am. J. Hum. Genet.* **84**, 351–366 (2009).

94. Chartier-Harlin, M.-C. et al. Alpha-synuclein locus duplication as a cause of familial Parkinson's disease. *Lancet* **364**, 1167–1169 (2004).
95. Valentine, J. S., Doucette, P. A. & Zittin Potter, S. Copper-zinc superoxide dismutase and amyotrophic lateral sclerosis. *Annu. Rev. Biochem.* **74**, 563–593 (2005).
96. Westermark, P., Andersson, A. & Westermark, G. T. Islet amyloid polypeptide, islet amyloid, and diabetes mellitus. *Physiol. Rev.* **91**, 795–826 (2011).
97. Sanchorawala, V. Light-chain (AL) amyloidosis: diagnosis and treatment. *Clin. J. Am. Soc. Nephrol.* **1**, 1331–1335 (2006).
98. Koch, K. M. Dialysis-related amyloidosis. *Kidney Int.* **41**, 1416–1429 (1992).
99. Li, X., Song, D. & Leng, S. X. Link between type 2 diabetes and Alzheimer's disease: from epidemiology to mechanism and treatment. *Clin. Interv. Aging* **10**, 549–560 (2015).
100. Uéda, K. et al. Molecular cloning of cDNA encoding an unrecognized component of amyloid in Alzheimer disease. *Proc. Natl Acad. Sci. USA* **90**, 11282–11286 (1993).
101. Maresova, P., Klimova, B., Novotny, M. & Kuca, K. Alzheimer's and Parkinson's diseases: Expected economic Impact on Europe-A call for a uniform European strategy. *J. Alzheimers Dis.* **54**, 1123–1133 (2016).
102. Li, J., Uversky, V. N. & Fink, A. L. Effect of familial Parkinson's disease point mutations A30P and A53T on the structural properties, aggregation, and fibrillation of human alpha-synuclein. *Biochemistry* **40**, 11604–11613 (2001).
103. Krone, M. G. et al. Effects of familial Alzheimer's disease mutations on the folding nucleation of the amyloid beta-protein. *J. Mol. Biol.* **381**, 221–228 (2008).
104. Mangione, P. P. et al. Structure, folding dynamics, and amyloidogenesis of D76N beta2-microglobulin: roles of shear flow, hydrophobic surfaces, and alpha-crystallin. *J. Biol. Chem.* **288**, 30917–30930 (2013).
105. Fan, H.-C. et al. Polyglutamine (PolyQ) diseases: genetics to treatments. *Cell Transplant.* **23**, 441–458 (2014).
106. Scheuermann, T. et al. Trinucleotide expansions leading to an extended poly-L-alanine segment in the poly (A) binding protein PABPN1 cause fibril formation. *Protein Sci.* **12**, 2685–2692 (2003).
107. Brais, B. et al. Short GCG expansions in the PABP2 gene cause oculopharyngeal muscular dystrophy. *Nat. Genet.* **18**, 164–167 (1998).
108. Renton, A. E. et al. A hexanucleotide repeat expansion in C9ORF72 is the cause of chromosome 9p21-linked ALS-FTD. *Neuron* **72**, 257–268 (2011).
109. DeJesus-Hernandez, M. et al. Expanded GGGGCC hexanucleotide repeat in noncoding region of C9ORF72 causes chromosome 9p-linked FTD and ALS. *Neuron* **72**, 245–256 (2011).
110. Budworth, H. & McMurray, C. T. A brief history of triplet repeat diseases. *Methods. Mol. Biol.* **1010**, 3–17 (2013).
111. Wiltfang, J. et al. Amyloid beta peptide ratio 42/40 but not Aβ 42 correlates with phospho-Tau in patients with low- and high-CSF Aβ 40 load. *J. Neurochem.* **101**, 1053–1059 (2007).
112. Ramella, N. A. et al. Human apolipoprotein A-I-derived amyloid: its association with atherosclerosis. *PLOS One* **6**, e22532 (2011).
113. Chiti, F. et al. A partially structured species of beta 2-microglobulin is significantly populated under physiological conditions and involved in fibrillogenesis. *J. Biol. Chem.* **276**, 46714–46721 (2001).
114. Eichner, T. & Radford, S. E. A generic mechanism of β2-microglobulin amyloid assembly at neutral pH involving a specific proline switch. *J. Mol. Biol.* **386**, 1312–1326 (2009).
115. Byers, B. et al. SNCA triplication Parkinson's patient's iPSC-derived DA neurons accumulate α-synuclein and are susceptible to oxidative stress. *PLOS One* **6**, e26159 (2011).
116. Lott, I. T. & Head, E. Alzheimer disease and Down syndrome: factors in pathogenesis. *Neurobiol. Aging* **26**, 383–389 (2005).
117. Scarpioni, R. et al. Dialysis-related amyloidosis: challenges and solutions. *Int. J. Nephrol. Renovasc. Dis.* **9**, 319–328 (2016).
118. Banani, S. F., Lee, H. O., Hyman, A. A. & Rosen, M. K. Biomolecular condensates: organizers of cellular biochemistry. *Nat. Rev. Mol. Cell Biol.* **18**, 285–298 (2017).
119. Wegmann, S. et al. Tau protein liquid-liquid phase separation can initiate tau aggregation. *EMBO J.* **37**, e98049 (2018).
120. Xiang, S. et al. The LC domain of hnRNPA2 adopts similar conformations in hydrogel polymers, liquid-like droplets, and nuclei. *Cell* **163**, 829–839 (2015).
121. Olzscha, H. et al. Amyloid-like aggregates sequester numerous metastable proteins with essential cellular functions. *Cell* **144**, 67–78 (2011).
122. Kovacs, G. G. & Budka, H. Prion diseases: from protein to cell pathology. *Am. J. Pathol.* **172**, 555–565 (2008).
123. Aguzzi, A. & Calella, A. M. Prions: protein aggregation and infectious diseases. *Physiol. Rev.* **89**, 1105–1150 (2009).
124. Aguzzi, A., Baumann, F. & Bremer, J. The prion's elusive reason for being. *Annu. Rev. Neurosci.* **31**, 439–477 (2008).
125. Botsios, S. & Manuelidis, L. CJD and scrapie require agent-associated nucleic acids for infection. *J. Cell. Biochem.* **117**, 1947–1958 (2016).
126. Wadsworth, J. D. F. et al. Kuru prions and sporadic Creutzfeldt–Jakob disease prions have equivalent transmission properties in transgenic and wild-type mice. *Proc. Natl Acad. Sci. USA* **105**, 3885–3890 (2008).
127. Cobb, N. J. & Surewicz, W. K. Prion diseases and their biochemical mechanisms. *Biochemistry* **48**, 2574–2585 (2009).
128. Wadsworth, J. D. F. et al. Tissue distribution of protease resistant prion protein in variant Creutzfeldt-Jakob disease using a highly sensitive immunoblotting assay. *Lancet* **358**, 171–180 (2001).
129. Masuda-Suzukake, M. et al. Prion-like spreading of pathological alpha-synuclein in brain. *Brain* **136**, 1128–1138 (2013).
130. Walker, L. C., Schelle, J. & Jucker, M. The prion-like properties of amyloid-β assemblies: implications for Alzheimer's disease. *Cold Spring Harb. Perspect. Med.* **6**, a024398 (2016).
131. An, L., Fitzpatrick, D. & Harrison, P. M. Emergence and evolution of yeast prion and prion-like proteins. *BMC Evol. Biol.* **16**, 24 (2016).
132. Alberti, S., Halfmann, R., King, O., Kapila, A. & Lindquist, S. A systematic survey identifies prions and illuminates sequence features of prionogenic proteins. *Cell* **137**, 146–158 (2009).
133. Sponarova, J., Nystrom, S. N. & Westermark, G. T. AA-amyloidosis can be transferred by peripheral blood monocytes. *PLOS One* **3**, e3308 (2008).
134. Solomon, A. et al. Amyloidogenic potential of foie gras. *Proc. Nat. Acad. Sci. USA* **104**, 10998–11001 (2007).
135. Knowles, T. P., Vendruscolo, M. & Dobson, C. M. The amyloid state and its association with protein misfolding diseases. *Nat. Rev. Mol. Cell. Biol.* **15**, 384–396 (2014).
136. Ferrone, F. Analysis of protein aggregation kinetics. *Methods Enzymol.* **309**, 256–274 (1999).
137. Sicorello, A. et al. Agitation and high ionic strength induce amyloidogenesis of a folded PDZ domain in native conditions. *Biophys. J.* **96**, 2289–2298 (2009).
138. Glabe, C. G. & Kayed, R. Common structure and toxic function of amyloid oligomers implies a common mechanism of pathogenesis. *Neurology* **66**, S74–S78 (2006).
139. Glabe, C. G. Common mechanisms of amyloid oligomer pathogenesis in degenerative disease. *Neurobiol. Aging* **27**, 570–575 (2006).
140. Meisl, G. et al. Molecular mechanisms of protein aggregation from global fitting of kinetic models. *Nat. Protoc.* **11**, 252–272 (2016).
141. Linse, S. Monomer-dependent secondary nucleation in amyloid formation. *Biophys. Rev.* **9**, 329–338 (2017).
142. Oosawa, F. & Asakura, S. *Thermodynamics of the Polymerization of Protein* (Academic Press, 1975).
143. Eaton, W. A. & Hofrichter, J. Hemoglobin S gelation and sickle cell disease. *Blood* **70**, 1245–1266 (1987).
144. Xue, W. F., Homans, S. W. & Radford, S. E. Systematic analysis of nucleation-dependent polymerization reveals new insights into the mechanism of amyloid self-assembly. *Proc. Natl Acad. Sci. USA* **105**, 8926–8931 (2008).
145. Cohen, S. I. A. et al. Proliferation of amyloid-β42 aggregates occurs through a secondary nucleation mechanism. *Proc. Natl Acad. Sci. USA* **110**, 9758–9763 (2013).
146. LeVine, H.r. Thioflavine T interaction with synthetic Alzheimer's disease beta-amyloid peptides: detection of amyloid aggregation in solution. *Protein. Sci.* **2**, 404–410 (1993).
147. Galvagnion, C. et al. Lipid vesicles trigger α-synuclein aggregation by stimulating primary nucleation. *Nat. Chem. Biol.* **11**, 229–234 (2015).
148. Buell, A. K. et al. Solution conditions determine the relative importance of nucleation and growth processes in α-synuclein aggregation. *Proc. Natl Acad. Sci. USA* **27**, 7671–7676 (2014).
149. Arosio, P. et al. Kinetic analysis reveals the diversity of microscopic mechanisms through which molecular chaperones suppress amyloid formation. *Nat. Commun.* **7**, 10948 (2016).
150. Habchi, J. et al. Systematic development of small molecules to inhibit specific microscopic steps of Abeta42 aggregation in Alzheimer's disease. *Proc. Natl Acad. Sci. USA* **114**, E200–E208 (2017).
151. Jackson, M. P. & Hewitt, E. W. Cellular proteostasis: degradation of misfolded proteins by lysosomes. *Essays Biochem.* **60**, 173–180 (2016).
152. Balchin, D., Hayer-Hartl, M. & Hartl, F. U. In vivo aspects of protein folding and quality control. *Science* **353**, aac4354 (2016).
153. Kim, Y. E., Hipp, M. S., Bracher, A., Hayer-Hartl, M. & Hartl, F. U. Molecular chaperone functions in protein folding and proteostasis. *Annu. Rev. Biochem.* **82**, 323–355 (2013).
154. Salminen, A. et al. Impaired autophagy and APP processing in Alzheimer's disease: the potential role of Beclin 1 interactome. *Prog. Neurobiol.* **106–107**, 33–54 (2013).
155. Winklhofer, K. F. & Haass, C. Mitochondrial dysfunction in Parkinson's disease. *Biochim. Biophys. Acta* **1802**, 29–44 (2010).
156. Uttara, B., Singh, A. V., Zamboni, P. & Mahajan, R. T. Oxidative stress and neurodegenerative diseases: a review of upstream and downstream antioxidant therapeutic options. *Curr. Neuropharmacol.* **7**, 65–74 (2009).
157. McLaurin, J. & Chakrabartty, A. Membrane disruption by Alzheimer β-amyloid peptides mediated through specific binding to either phospholipids or gangliosides. Implications for neurotoxicity. *J. Biol. Chem.* **25**, 26482–26489 (1996).
158. Goodchild, S. C. et al. β2-Microglobulin amyloid fibril-induced membrane disruption is enhanced by endosomal lipids and acidic pH. *PLOS One* **9**, e104492 (2014).
159. Nelson, P. T. et al. Correlation of Alzheimer disease neuropathologic changes with cognitive status: a review of the literature. *J. Neuropathol. Exp. Neurol.* **71**, 362–381 (2012).
160. Reixach, N., Deechongkit, S., Jiang, X., Kelly, J. W. & Buxbaum, J. N. Tissue damage in the amyloidoses: transthyretin monomers and non-native oligomers are the major cytotoxic species in tissue culture. *Proc. Natl Acad. Sci. USA* **101**, 2817–2822 (2004).
161. Baglioni, S. et al. Prefibrillar amyloid aggregates could be generic toxins in higher organisms. *J. Neurosci.* **26**, 8160–8167 (2006).
162. Bucciantini, M. et al. Inherent toxicity of aggregates implies a common mechanism for protein misfolding diseases. *Nature* **416**, 507–511 (2002).
163. Simoneau, S. et al. In vitro and in vivo neurotoxicity of prion protein oligomers. *PLOS Pathog.* **3**, e125 (2007).
164. Winner, B. et al. In vivo demonstration that α-synuclein oligomers are toxic. *Proc. Natl Acad. Sci. USA* **108**, 4194–4199 (2011).
165. Serra-Batiste, M. et al. Aβ42 assembles into specific beta-barrel pore-forming oligomers in membrane-mimicking environments. *Proc. Natl Acad. Sci. USA* **113**, 10866–10871 (2016).
166. Evangelisti, E. et al. Binding affinity of amyloid oligomers to cellular membranes is a generic indicator of cellular dysfunction in protein misfolding diseases. *Sci. Rep.* **6**, 32721 (2016).
167. Pfefferkorn, C. M., Jiang, Z. & Lee, J. C. Biophysics of α-synuclein membrane interactions. *Biochim. Biophys. Acta* **1818**, 162–171 (2012).
168. Lashuel, H. A. et al. α-Synuclein, especially the Parkinson's disease-associated mutants, forms pore-like annular and tubular protofibrils. *J. Mol. Biol.* **322**, 1089–1102 (2002).
169. Lesné, S. et al. A specific amyloid-β protein assembly in the brain impairs memory. *Nature* **440**, 352–357 (2006).
170. Shankar, G. M. et al. Amyloid-beta protein dimers isolated directly from Alzheimer's brains impair synaptic plasticity and memory. *Nat. Med.* **14**, 837–842 (2008).
171. Fusco, G. et al. Structural basis of membrane disruption and cellular toxicity by α-synuclein oligomers. *Science* **358**, 1440–1443 (2017).
172. Tosatto, L. et al. Single-molecule FRET studies on α-synuclein oligomerization of Parkinson's disease genetically related mutants. *Sci. Rep.* **5**, 16696 (2015).

173. Chiti, F. & Dobson, C. M. Amyloid formation by globular proteins under native conditions. *Nat. Chem. Biol.* **5**, 15–22 (2009).
174. Tsigelny, I. F. et al. Role of α-synuclein penetration into the membrane in the mechanisms of oligomer pore formation. *FEBS J.* **279**, 1000–1013 (2012).
175. Young, L. M., Cao, P., Raleigh, D. P., Ashcroft, A. E. & Radford, S. E. Ion mobility spectrometry-mass spectrometry defines the oligomeric intermediates in amylin amyloid formation and the mode of action of inhibitors. *J. Am. Chem. Soc.* **136**, 660–670 (2014).
176. Young, L. M., Tu, L. H., Raleigh, D. P., Ashcroft, A. E. & Radford, S. E. Understanding co-polymerization in amyloid formation by direct observation of mixed oligomers. *Chem. Sci.* **8**, 5030–5040 (2017).
177. Tipping, K. W., van Oosten-Hawle, P., Hewitt, E. W. & Radford, S. E. Amyloid fibres: inert end-stage aggregates or key players in disease? *Trends Biochem. Sci.* **40**, 719–727 (2015).
178. Milanesi, L. et al. Direct three-dimensional visualization of membrane disruption by amyloid fibrils. *Proc. Natl Acad. Sci. USA* **109**, 20455–20460 (2012).
179. Phelan, M. M., Caamaño-Gutiérrez, E., Gant, M. S., Grosman, R. X. & Madine, J. Using an NMR metabolomics approach to investigate the pathogenicity of amyloid-beta and alpha-synuclein. *Metabolomics* **13**, 151 (2017).
180. Gharibyan, A. L. et al. Lysozyme amyloid oligomers and fibrils induce cellular death via different apoptotic/necrotic pathways. *J. Mol. Biol.* **365**, 1337–1349 (2007).
181. Grudzielanek, S. et al. Cytotoxicity of insulin within its self-assembly and amyloidogenic pathways. *J. Mol. Biol.* **370**, 372–384 (2007).
182. Novitskaya, V., Bocharova, O. V., Bronstein, I. & Baskakov, I. V. Amyloid fibrils of mammalian prion protein are highly toxic to cultured cells and primary neurons. *J. Biol. Chem.* **281**, 13828–13836 (2006).
183. Berthelot, K., Ta, H. P., Gêan, J., Lecomte, S. & Cullin, C. In vivo and in vitro analyses of toxic mutants of HET-S: FTIR antiparallel signature correlates with amyloid toxicity. *J. Mol. Biol.* **412**, 137–152 (2011).
184. Lee, Y. J., Savtchenko, R., Ostapchenko, V. G., Makarava, N. & Baskakov, I. V. Molecular structure of amyloid fibrils controls the relationship between fibrillar size and toxicity. *PLOS One* **6**, e20244 (2011).
185. Mossuto, M. F. et al. Disulfide bonds reduce the toxicity of the amyloid fibrils formed by an extracellular protein. *Angew. Chem. Int. Ed. Engl.* **50**, 7048–7051 (2011).
186. Makarava, N. et al. Recombinant prion protein induces a new transmissible prion disease in wild-type animals. *Acta Neuropathol.* **119**, 177–187 (2010).
187. Qiang, W., Kelley, K. & Tycko, R. Polymorph-specific kinetics and thermodynamics of beta-amyloid fibril growth. *J. Am. Chem. Soc.* **135**, 6860–6871 (2013).
188. Stewart, K. L., Hughes, E., Yates, E. A., Middleton, D. A. & Radford, S. E. Molecular origins of the compatibility between glycosaminoglycans and Aβ40 amyloid fibrils. *J. Mol. Biol.* **429**, 2449–2462 (2017).
189. Cohen, M. L. et al. Rapidly progressive Alzheimer's disease features distinct structures of amyloid-beta. *Brain* **138**, 1009–1022 (2015).
190. Tipping, K. W. et al. pH-induced molecular shedding drives the formation of amyloid fibril-derived oligomers. *Proc. Natl Acad. Sci. USA* **112**, 5691–5696 (2015).
191. Serra-Vidal, B. et al. Hydrogen/deuterium exchange-protected oligomers populated during Abeta fibril formation correlate with neuronal cell death. *ACS Chem. Biol.* **9**, 2678–2685 (2014).
192. Pilla, E., Schneider, K. & Bertolotti, A. Coping with protein quality control failure. *Annu. Rev. Cell. Dev. Biol.* **33**, 439–465 (2017).
193. Schneider, K. & Bertolotti, A. Surviving protein quality control catastrophes—from cells to organisms. *J. Cell Sci.* **128**, 3861–3869 (2015).
194. Walther, D. M. et al. Widespread proteome remodeling and aggregation in aging *C. elegans*. *Cell* **161**, 919–932 (2015).
195. Ciryam, P., Kundra, R., Morimoto, R. I., Dobson, C. M. & Vendruscolo, M. Supersaturation is a major driving force for protein aggregation in neurodegenerative diseases. *Trends Pharmacol. Sci.* **36**, 72–77 (2015).
196. Kundra, R., Ciryam, P., Morimoto, R. I., Dobson, C. M. & Vendruscolo, M. Protein homeostasis of a metastable subproteome associated with Alzheimer's disease. *Proc. Natl Acad. Sci. USA* **114**, E5703–E5711 (2017).
197. Bonar, L., Cohen, A. S. & Skinner, M. M. Characterization of the amyloid fibril as a cross-beta protein. *Proc. Soc. Exp. Biol. Med.* **131**, 1373–1375 (1969).
198. Blake, C. & Serpell, L. C. Synchrotron X-ray studies suggest that the core of the transthyretin amyloid fibril is a continuous β-sheet helix. *Structure* **4**, 989–998 (1996).
199. Serpell, L. C. & Smith, J. M. Direct visualisation of the β-sheet structure of synthetic Alzheimer's amyloid. *J. Mol. Biol.* **299**, 225–231 (2000).
200. Jahn, T. R., Tennent, G. A. & Radford, S. E. A common beta-sheet architecture underlies in vitro and in vivo β-2-microglobulin amyloid fibrils. *J. Biol. Chem.* **283**, 17279–17286 (2008).
201. Zandomeneghi, G., Krebs, M. R., McCammon, M. G. & Fandrich, M. FTIR reveals structural differences between native β-sheet proteins and amyloid fibrils. *Protein. Sci.* **13**, 3314–3321 (2004).
202. Sarroukh, R., Goormaghtigh, E., Ruysschaert, J. M. & Raussens, V. ATR-FTIR: a "rejuvenated" tool to investigate amyloid proteins. *Biochim. Biophys. Acta* **1828**, 2328–2338 (2013).
203. Adler-Abramovich, L. et al. Phenylalanine assembly into toxic fibrils suggests amyloid etiology in phenylketonuria. *Nat. Chem. Biol.* **8**, 701–706 (2012).
204. Julien, O. et al. Unraveling the mechanism of cell death induced by chemical fibrils. *Nat. Chem. Biol.* **10**, 969–976 (2014).
205. Lazar, K. L., Miller-Auer, H., Getz, G. S., Orgel, J. P. R. O. & Meredith, S. C. Helix-turn-helix peptides that form alpha-helical fibrils: turn sequences drive fibril structure. *Biochemistry* **44**, 12681–12689 (2005).
206. Tayeb-Fligelman, E. et al. The cytotoxic *Staphylococcus aureus* PSMα3 reveals a cross-α amyloid-like fibril. *Science* **355**, 831–833 (2017).
207. Sangwan, S. et al. Atomic structure of a toxic, oligomeric segment of SOD1 linked to amyotrophic lateral sclerosis (ALS). *Proc. Natl Acad. Sci. USA* **114**, 8770–8775 (2017).
208. Laganowsky, A. et al. Atomic view of a toxic amyloid small oligomer. *Science* **335**, 1228–1231 (2012).
209. Shirahama, T. & Cohen, A. S. Structure of amyloid fibrils after negative staining and high-resolution electron microscopy. *Nature* **206**, 737–738 (1965).
210. Tattum, M. H. et al. Elongated oligomers assemble into mammalian PrP amyloid fibrils. *J. Mol. Biol.* **357**, 975–985 (2006).
211. White, H. E. et al. Globular tetramers of β(2)-microglobulin assemble into elaborate amyloid fibrils. *J. Mol. Biol.* **389**, 48–57 (2009).
212. Paravastua, A. K., Leapman, R. D., Yau, W. & Tycko, R. Molecular structural basis for polymorphism in Alzheimer's β-amyloid fibrils. *Proc. Natl Acad. Sci. USA* **105**, 18349–18354 (2008).
213. Lu, J. X. et al. Molecular structure of beta-amyloid fibrils in Alzheimer's disease brain tissue. *Cell* **154**, 1257–1268 (2013).
214. Kajava, A. V., Baxa, U., Wickner, R. B. & Steven, A. C. A model for Ure2p prion filaments and other amyloids: the parallel superpleated beta-structure. *Proc. Natl Acad. Sci. USA* **101**, 7885–7890 (2004).
215. Kajava, A. V., Aebi, U. & Steven, A. C. The parallel superpleated β-structure as a model for amyloid fibrils of human amylin. *J. Mol. Biol.* **348**, 247–252 (2005).
216. Tuttle, M. D. et al. Solid-state NMR structure of a pathogenic fibril of full-length human alpha-synuclein. *Nat. Struct. Mol. Biol.* **23**, 409–415 (2016).
217. Marshall, K. E. et al. Characterizing the assembly of the Sup35 yeast prion fragment, GNNQQNY: structural changes accompany a fiber-to-crystal switch. *Biophys. J.* **98**, 330–338 (2010).
218. Reynolds, N. P. et al. Competition between crystal and fibril formation in molecular mutations of amyloidogenic peptides. *Nat. Commun.* **8**, 1338 (2017).
219. Saracino, G. A., Villa, A., Moro, G., Cosentino, U. & Salmona, M. Spontaneous beta-helical fold in prion protein: the case of PrP(82–146). *Proteins* **75**, 964–976 (2009).
220. Kajava, A. V. & Steven, A. C. β-rolls, β-helices, and other β-solenoid proteins. *Adv. Protein Chem.* **73**, 55–96 (2006).
221. Peng, Z., Peralta, M. D. R. & Toney, M. D. Extraordinarily stable amyloid fibrils engineered from structurally defined beta-solenoid proteins. *Biochemistry* **56**, 6041–6050 (2017).
222. Wolfram, F. et al. Catalytic mechanism and mode of action of the periplasmic alginate epimerase AlgG. *J. Biol. Chem.* **289**, 6006–6019 (2014).
223. Leinala, E. K., Davies, P. L. & Jia, Z. Crystal structure of beta-helical antifreeze protein points to a general ice binding model. *Structure* **10**, 619–627 (2002).
224. Muller, J. J. et al. An intersubunit active site between supercoiled parallel beta helices in the trimeric tailspike endorhamnosidase of *Shigella flexneri* Phage Sf6. *Structure* **16**, 766–775 (2008).
225. Kajava, A. V., Baxa, U. & Steven, A. C. Beta arcades: recurring motifs in naturally occurring and disease-related amyloid fibrils. *FASEB J.* **24**, 1311–1319 (2010).
226. Ritter, C. et al. Correlation of structural elements and infectivity of the HET-s prion. *Nature* **435**, 844–848 (2005).
227. Bousset, L. et al. Structural and functional characterization of two alpha-synuclein strains. *Nat. Commun.* **4**, 2575 (2013).
228. Goldsbury, C. S. et al. Polymorphic fibrillar assembly of human amylin. *J. Struct. Biol.* **119**, 17–21 (1997).
229. Jiménez, J. et al. The protofilament structure of insulin amyloid fibrils. *Proc. Natl Acad. Sci. USA* **99**, 9196–9201 (2002).
230. Dearborn, A. D. et al. Alpha-synuclein amyloid fibrils with two entwined, asymmetrically associated protofibrils. *J. Biol. Chem.* **291**, 2310–2318 (2016).
231. Andersen, C. B. et al. Glucagon fibril polymorphism reflects differences in protofilament backbone structure. *J. Mol. Biol.* **397**, 932–946 (2010).
232. Xiao, Y. et al. Aβ(1–42) fibril structure illuminates self-recognition and replication of amyloid in Alzheimer's disease. *Nat. Struct. Mol. Biol.* **22**, 499–505 (2015).
233. Chen, B., Thurber, K. R., Shewmaker, F., Wickner, R. B. & Tycko, R. Measurement of amyloid fibril mass-per-length by tilted-beam transmission electron microscopy. *Proc. Natl Acad. Sci. USA* **106**, 14339–14344 (2009).
234. Doussineau, T. et al. Mass determination of entire amyloid fibrils by using mass spectrometry. *Angew. Chem. Int. Ed. Engl.* **55**, 2340–2344 (2016).
235. Crick, F. H. C. & Rich, A. Structure of polyglyciene II. *Nature* **176**, 780–781 (1955).
236. Lee, M. et al. Zinc-binding structure of a catalytic amyloid from solid-state NMR. *Proc. Natl Acad. Sci. USA* **114**, 6191–6196 (2017).
237. Viles, J. H. Metal ions and amyloid fiber formation in neurodegenerative diseases. Copper, zinc and iron in Alzheimer's, Parkinson's and prion diseases. *Coords. Chem. Rev.* **256**, 2271–2284 (2012).
238. Gath, J. et al. Yet another polymorph of α-synuclein: solid-state sequential assignments. *Biomol. NMR Assign.* **8**, 395–404 (2014).
239. Gath, J. et al. Unlike twins: an NMR comparison of two α-synuclein polymorphs featuring different toxicity. *PLOS One* **9**, e90659 (2014).
240. Anfinsen, C. Principals that govern the folding of protein chains. *Science* **181**, 223–230 (1973).
241. Sidhu, A., Segers-Nolten, I., Raussens, V., Claessens, M. M. & Subramaniam, V. Distinct mechanisms determine α-synuclein fibril morphology during growth and maturation. *ACS Chem. Neurosci.* **8**, 538–547 (2017).
242. Eichner, T. & Radford, S. E. A diversity of assembly mechanisms of a generic amyloid fold. *Mol. Cell* **43**, 8–18 (2011).
243. Weissmann, C. & Flechsig, E. PrP knock-out and PrP transgenic mice in prion research. *Br. Med. Bull.* **66**, 43–60 (2003).
244. Geschwind, M. D. Prion diseases. *Continuum (Minneap. Minn.)* **21**, 1612–1638 (2015).
245. Kitazawa, M., Medeiros, R. & LaFerla, F. M. Transgenic mouse models of Alzheimer disease: developing a better model as a tool for therapeutic interventions. *Curr. Pharm. Des.* **18**, 1131–1147 (2012).
246. Khalaf, O. et al. The H50Q mutation enhances α-synuclein aggregation, secretion, and toxicity. *J. Biol. Chem.* **289**, 21856–21876 (2014).
247. Appel-Cresswell, S. et al. Alpha-synuclein p. H50Q, a novel pathogenic mutation for Parkinson's disease. *Mov. Disord.* **28**, 811–813 (2013).
248. Lesage, S. et al. G51D α-synuclein mutation causes a novel parkinsonian-pyramidal syndrome. *Ann. Neurol.* **73**, 459–471 (2013).
249. Nielsen, S. B. et al. Wildtype and A30P mutant α-synuclein form different fibril structures. *PLOS One* **8**, e67713 (2013).
250. Petrucci, S., Ginevrino, M. & Valente, E. M. Phenotypic spectrum of α-synuclein mutations: New insights from patients and cellular models. *Parkinsonism Relat. Disord.* **22** (Suppl. 1), S16–S20 (2016).
251. Schutz, A. K. et al. Atomic-resolution three-dimensional structure of amyloid beta fibrils bearing the Osaka mutation. *Angew. Chem. Int. Ed. Engl.* **54**, 331–335 (2015).
252. Andresen, J. M. et al. The relationship between CAG repeat length and age of onset differs for Huntington's disease patients with juvenile onset or adult onset. *Ann. Hum. Genet.* **71**, 295–301 (2007).

253. Petkova, A. T. et al. Self-propagating, molecular-level polymorphism in Alzheimer's β-amyloid fibrils. *Science* **307**, 262–265 (2005).
254. Stöhr, j. et al. Purified and synthetic Alzheimer's amyloid beta (Aβ) prions. *Proc. Natl Acad. Sci. USA* **109**, 11025–11030 (2012).
255. Meyer-Luehmann, M. et al. Exogenous induction of cerebral β-amyloidogenesis is governed by agent and host. *Science* **313**, 1781–1784 (2006).
256. Liu, J. et al. Amyloid structure exhibits polymorphism on multiple length scales in human brain tissue. *Sci. Rep.* **6**, 33079 (2016).
257. Nyström, S. et al. Evidence for age-dependent in vivo conformational rearrangement within Aβ amyloid deposits. *ACS Chem. Biol* **8**, 1128–1133 (2013).
258. Perez-Nievas, B. G. et al. Dissecting phenotypic traits linked to human resilience to Alzheimer's pathology. *Brain* **136**, 2510–2526 (2013).
259. Elman, J. A. et al. Neural compensation in older people with brain amyloid-beta deposition. *Nat. Neurosci.* **17**, 1316–1318 (2014).
260. Strømland, Ø., Jakubec, M., Furse, S. & Halskau, Ø. Detection of misfolded protein aggregates from a clinical perspective. *J. Clin. Transl Res.* **2**, 11–26 (2016).
261. Bulawa, C. E. et al. Tafamidis, a potent and selective transthyretin kinetic stabilizer that inhibits the amyloid cascade. *Proc. Natl Acad. Sci. USA* **109**, 9629–9634 (2012).
262. Ludtmann, M. H. et al. Monomeric alpha-synuclein exerts a physiological role on brain ATP synthase. *J. Neurosci.* **36**, 10510–10521 (2016).
263. Pearson, H. A. & Peers, C. Physiological roles for amyloid beta peptides. *J. Physiol.* **575**, 5–10 (2006).
264. Barucker, C. et al. Abeta42-oligomer interacting peptide (AIP) neutralizes toxic amyloid-beta42 species and protects synaptic structure and function. *Sci. Rep.* **5**, 15410 (2015).
265. Du, W. J. et al. Brazilin inhibits amyloid beta-protein fibrillogenesis, remodels amyloid fibrils and reduces amyloid cytotoxicity. *Sci. Rep.* **5**, 7992 (2015).
266. Jarosz-Griffiths, H. H., Noble, E., Rushworth, J. V. & Hooper, N. M. Amyloid-beta receptors: the good, the bad, and the prion protein. *J. Biol. Chem.* **291**, 3174–3183 (2016).
267. Mao, X. et al. Pathological α-synuclein transmission initiated by binding lymphocyte-activation gene 3. *Science* **353**, aah3374 (2016).
268. Verma, M., Vats, A. & Taneja, V. Toxic species in amyloid disorders: Oligomers or mature fibrils. *Ann. Indian Acad. Neurol.* **18**, 138–145 (2015).
269. Berry, D. B. et al. Drug resistance confounding prion therapeutics. *Proc. Natl Acad. Sci. USA Proc. Natl Acad. Sci. USA* **110**, E4160–E4169 (2013).
270. Li, J., Browning, S., Mahal, S. P., Oelschlegel, A. M. & Weissmann, C. Darwinian evolution of prions in cell culture. *Science* **327**, 869–872 (2010).
271. Oelschlegel, A. M. & Weissmann, C. Acquisition of drug resistance and dependence by prions. *PLOS Pathog.* **9**, e1003158 (2013).
272. Seidler, P. M. et al. Structure-based inhibitors of tau aggregation. *Nat. Chem.* **10**, 170–176 (2018).
273. Sievers, S. A. et al. Structure-based design of non-natural amino-acid inhibitors of amyloid fibril formation. *Nature* **475**, 96–100 (2011).
274. Jiang, L. et al. Structure-based discovery of fiber-binding compounds that reduce the cytotoxicity of amyloid beta. *eLife* **2**, e00857 (2013).
275. Kad, N. M. et al. Hierarchical assembly of β2-microglobulin amyloid in vitro revealed by atomic force microscopy. *J. Mol. Biol.* **330**, 785–797 (2003).
276. Watanabe-Nakayama, T. et al. High-speed atomic force microscopy reveals structural dynamics of amyloid beta1-42 aggregates. *Proc. Natl Acad. Sci. USA* **113**, 5835–5840 (2016).
277. Silvers, R. et al. Aggregation and fibril structure of AβMO1-42 and Aβ1-42. *Biochemistry* **56**, 4850–4859 (2017).
278. Colvin, M. T. et al. Atomic resolution structure of monomorphic Aβ42 amyloid fibrils. *J. Am. Chem. Soc.* **138**, 9663–9674 (2016).
279. Schütz, A. K. et al. Binding of polythiophenes to amyloids: structural mapping of the pharmacophore. *ACS Chem. Neurosci.* **9**, 475–481 (2017).
280. Ries, J. et al. Superresolution imaging of amyloid fibrils with binding-activated probes. *ACS Chem. Neurosci.* **4**, 1057–1061 (2013).
281. Choi, J. H., May, B. C., Wille, H. & Cohen, F. E. Molecular modeling of the misfolded insulin subunit and amyloid fibril. *Biophys. J.* **97**, 3187–3195 (2009).
282. Ladner, C. L. et al. Stacked sets of parallel, in-register beta-strands of beta2-microglobulin in amyloid fibrils revealed by site-directed spin labeling and chemical labeling. *J. Biol. Chem.* **285**, 17137–17147 (2010).
283. Zhang, Y. et al. Pulsed hydrogen-deuterium exchange mass spectrometry probes conformational changes in amyloid beta (Abeta) peptide aggregation. *Proc. Natl Acad. Sci. USA* **110**, 14604–14609 (2013).
284. Der-Sarkissian, A., Jao, C. C., Chen, J. & Langen, R. Structural organization of alpha-synuclein fibrils studied by site-directed spin labeling. *J. Biol. Chem.* **278**, 37530–37535 (2003).
285. Varkey, J. & Langen, R. Membrane remodeling by amyloidogenic and non-amyloidogenic proteins studied by EPR. *J. Magn. Reson.* **280**, 127–139 (2017).
286. Cohen, A. S. & Calkins, E. Electron microscopic observations on a fiberous component in amyloid of diverse origins. *Nature* **183**, 1202–1203 (1959).
287. Cohen, A. S. & Shirahama, T. High resolution electron microscopic analysis of the amyloid fibril. *J. Cell Bio.* **33**, 679 (1967).
288. Astbury, W. T. X-ray studies of protein structure. *Cold Spring Harb. Symp. Quant. Biol.* **2**, 15–27 (1934).
289. Jimenez, J. L., Tennent, G., Pepys, M. & Saibil, H. R. Structural diversity of ex vivo amyloid fibrils studied by cryo-electron microscopy. *J. Mol. Biol.* **311**, 241–247 (2001).
290. Schaffer, J. et al. Recombinant versus natural human 111In-beta2-microglobulin for scintigraphic detection of Abeta2m amyloid in dialysis patients. *Kidney Int.* **58**, 873–880 (2000).
291. Pras, M., Schubert, M., Zucker-Franklin, D., Rimon, A. & Franklin, E. C. The characterization of soluble amyloid prepared in water. *J. Clin. Invest.* **47**, 924–933 (1968).
292. Fändrich, M. & Dobson, C. M. The behaviour of polyamino acids reveals an inverse side chain effect in amyloid structure formation. *EMBO J.* **21**, 5682–5690 (2002).
293. Sikorski, P. & Atkins, E. New model for crystalline polyglutamine assemblies and their connection with amyloid fibrils. *Biomacromolecules* **6**, 425–432 (2005).
294. Ranson, N., Stromer, T., Bousset, L., Melki, R. & Serpell, L. C. Insights into the architecture of the Ure2p yeast protein assemblies from helical twisted fibrils. *Protein Sci.* **15**, 2481–2487 (2006).
295. Graeber, M. B., Kösel, S., Grasbon-Frodl, E., Möller, H. J. & Mehraein, P. Histopathology and APOE genotype of the first Alzheimer disease patient, Auguste D. *Neurogenetics* **1**, 223–228 (1998).
296. Nicoll, A. J. et al. Amyloid-beta nanotubes are associated with prion protein-dependent synaptotoxicity. *Nat. Commun.* **4**, 2416 (2013).
297. Martins, I. C. et al. Lipids revert inert Aβ amyloid fibrils to neurotoxic protofibrils that affect learning in mice. *EMBO J.* **27**, 224–233 (2008).
298. Jakhria, T. et al. beta2-microglobulin amyloid fibrils are nanoparticles that disrupt lysosomal membrane protein trafficking and inhibit protein degradation by lysosomes. *J. Biol. Chem.* **289**, 35781–35794 (2014).
299. Fujioka, S. et al. Update on novel familial forms of Parkinson's disease and multiple system atrophy. *Parkinsonism Relat. Disord.* **20**, S29–S34 (2014).
300. Pagano, G., Ferrara, N., Brooks, D. J. & Pavese, N. Age at onset and Parkinson disease phenotype. *Neurology* **86**, 1400–1407 (2016).

Acknowledgements
The authors thank members of their laboratories and their colleagues for many helpful discussions while preparing this Review. M.G.I., M.P.J., E.W.H., N.A.R and S.E.R. acknowledge funding from the European Research Council (ERC) under the European Union's Seventh Framework Programme (FP7/2007-2013) ERC grant agreement no. 322408 and from the Wellcome Trust (092896MA and 204963).

Author contributions
All authors wrote the manuscript.

Competing interests
The authors declare no competing interests.

Publisher's note
Springer Nature remains neutral with regard to jurisdictional claims in published maps and institutional affiliations.

RELATED LINKS
Protein Data Bank: http://www.rcsb.org/pdb/home/home.do